Responsive Organoboranes with Dynamic Conformation of Octacyclophane-Type Scaffolds: Synthesis, AIE and Temperature-Dependent Dual Emissions

Kai Zhang,[a] Guangqian Ji,[a] Niu Zhang,*[b] Nan Wang,[a] Xiaodong Yin,[a] Quansong Li,[a] and Pangkuan Chen*[a]

[a] Beijing Key Laboratory of Photoelectronic/Electrophotonic Conversion Materials, Key Laboratory of Cluster Science of the Ministry of Education, School of Chemistry and Chemical Engineering, Beijing Institute of Technology of China, Beijing, 102488, China

[b] Analysis & Testing Centre, Beijing Institute of Technology of China, Beijing, 102488, China

1. Experimental Section

Materials and General Methods: Dibenzosuberone, 4-(diphenylamino)-phenylboronic acid, potassium carbonate, tetrakis(triphenylphosphine)palladium, trifluoroacetic acid, sodium tert-butoxide, stannous chloride, copper(II) bromide, aluminum chloride and iodine were purchased from Energy Chemical. Tetrahydrofuran (THF), dichloromethane, petroleum ether, methanol, and ethyl acetate were purchased from Sinopharm Chemical Reagent Co., Ltd. The chemicals were used without further purification unless otherwise noted. Anhydrous solvent was distilled from commercial solvent with sodium/benzopheneone. All commercial chemicals were used without further purification. 3,7-dinitro-dibenzosuberone (**1**), 3,7-diaminodibenzosuberone (**2**), 3,7-dibromo-5-methylene-10,11-dihydro-5H-dibenzo[a,d][7]annulene (**3**), and 2-(4-(dimesitylboranyl)phenyl)-4,4,5,5-tetra-methyl-1,3,2-dioxaborolane were prepared using the similar procedures previously described[1, 2].

400 MHz ^{1}H, 101 MHz ^{13}C, and 225 MHz ^{11}B NMR spectra were recorded on a Bruker spectrometer. ^{11}B NMR spectra were acquired with boron-free quartz NMR tubes and the spectra were referenced externally to $BF_3 \cdot Et_2O$ ($\delta = 0$). High resolution mass spectral data were obtained via ESI on an Agilent (Q-TOF 6520) analyzer.

UV-visible absorption spectra were recorded on a Cary 300 UV-Vis spectrophotometer. Luminescent spectra were recorded on an Edinburgh Instruments FLS980. Fluorescent quantum efficiencies were determined using a Hamamatsu C11347-11 Quantaurus-QY spectrometer.

Electrochemical measurements were conducted on an AUTOLAB-CV-75W analyzer with a scan rate of 100 mV/s. The electrochemical cell was a standard three-compartment cell composed of a glass carbon working electrode, a Pt auxiliary

electrode, and a Pt wire reference electrode. All tests were performed using [Bu_4N][PF_6] (0.1 M) as the supporting electrolyte. The voltammograms were obtained in anhydrous and nitrogen saturated CH_2Cl_2 or THF solutions. The potentials are reported relative to the ferrocene/ferrocenium couple.

X-ray single crystals were obtained on a Bruker D8 X-ray single crystal Venture diffractometer. SAINT5.0 and SADABS programs are used for the reduction and absorption correction of crystal data. The resolution and refinement of the crystal structure are obtained on the SHELXTL-97 software. Using the direct or Patterson methods, all nonhydrogen source coordinates are obtained by using the differential Fourier method and the least square method. Then the geometric method and the difference value are used. The hydrogen atom coordinates were obtained by Fourier method, and the crystal structure was obtained. The CCDC number of 2069496 is deposited.

Femtosecond transient absorption measurements were performed with Ti:sapphire regenerative amplifier (Legend Elite HE+USX-1K-II, 800 nm, 25 fs, 1 kHz). While the second harmonic of the output (330 nm) was used as a pump light. A white-light continuum generated by focusing a fundamental of the regenerative amplifier was used as a probe light (400-1600 nm). The probe light passed through the sample cell was dispersed by a grating and its spectrum was imaged onto a linear image sensor. The transient absorption spectra were recorded as a function of the pump-probe delay.

DFT calculations were performed with the Gaussian 09 program. Geometry optimizations and vertical excitations were calculated by means of hybrid density functional B3LYP and CAM-B3LYP with the basis set of 6-31G*. The input files and orbital representations were generated with Gaussview 5.0 (scaling radii of 75%, isovalue = 0.02). Excitation data were calculated using TD-DFT (B3LYP/6-311G** and CAM-B3LYP/6-311G**). The resulting structures were confirmed to be stationary points through vibrational frequency analysis.

2. Synthetic Procedures

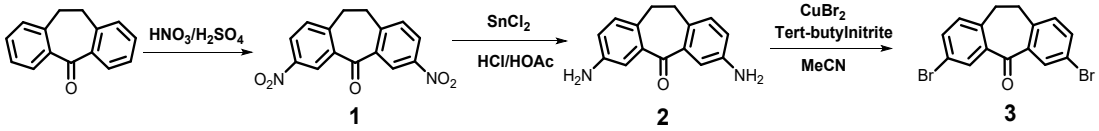

Compounds **1**, **2** and **3** were prepared by previously reported procedures.[1]

2.1 Synthesis of 4

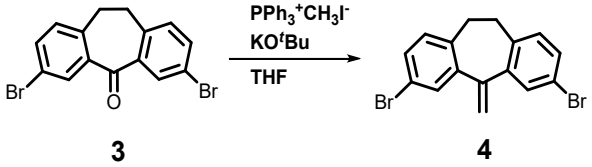

Methyltriphenylphosphonium iodide (0.29 g, 0.72 mmol) was added to a dry Schlenk tube. After deoxygenation by freeze−pump−thawing procedure, dry THF (10 mL) was added via syringe and gave a milky white suspension. At room temperature, KO^{t}Bu (80 mg, 0.72 mmol) was then added to the suspension with stirring, and a bright yellow methylenetriphenylphosphorane ylide was generated. After stirring for 20 min, **3** (0.20 g, 0.60 mmol) in THF was slowly added via syringe. The reaction was stirred at 40 °C for 12 h and then filtrated through a flash column of silica gel with CH_2Cl_2 as eluent to remove unreacted base. The concentrated raw product was further purified via column chromatography on silica gel using petroleum ether (PE) as eluent to give **4** (0.16 g, yield: 80%) as a white powder. ^{1}H NMR (400 MHz, acetone-d_6) ^{1}H NMR (400 MHz, $CDCl_3$) δ 7.47 (d, J = 2.0 Hz, 2H), 7.32 (dd, J = 8.0, 2.0 Hz, 2H), 6.98 (d, J = 8.0 Hz, 2H), 5.45 (s, 2H), 3.06 (s, 4H). ^{13}C NMR (101 MHz, $CDCl_3$) δ 149.2, 142.3, 137.1, 130.8, 130.7, 130.6, 119.7, 119.1, 32.5. GC-MS (m/z): calcd. for $C_{21}H_{12}Br_2O_2$ [M^+] 363.9, found 363.9.

2.2 Synthesis of 5

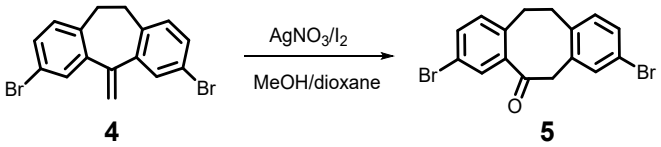

Silver nitrate (0.94 g, 5.53 mmol) was fully dissolved in refluxing methanol (20 mL) in a 100 mL round bottom flask. I_2 (0.35 g, 2.76 mmol) was added together with **4** (0.5 g, 1.37 mmol) in 1, 4-dioxane (20 mL), leading to precipitates of AgI salt immediately. The reaction mixture was refluxed with stirring for 24 h. After cooling to r.t., the solid byproduct was filtered off and the filtrate evaporated under reduced pressure. The crude product was purified by column chromatography on silica gel using

CH_2Cl_2/PE (1/3, v/v) as eluent to yield **5** (0.34 g, yield: 65%) as a white powder. ^{1}H NMR (400 MHz, $CDCl_3$) δ 7.53 (d, *J* = 4.0 Hz, 1H), 7.35–7.44 (m, 1H), 7.23–7.14 (m, 2H), 6.97 (d, *J* = 8.0 Hz, 1H), 6.86 (d, *J* = 8.0 Hz, 1H), 4.08 (s, 2H), 3.33–3.10 (m, 4H).^{13}C NMR (101 MHz, $CDCl_3$) δ 201.9, 140.1, 137.2, 136.4, 135.3, 134.6, 133.4, 132.6, 131.5, 131.1, 130.8, 120.8, 120.4, 77.4, 50.8, 34.0, 33.1. GC-MS (m/z): calcd. for $C_{21}H_{12}Br_2O_2$ [M^+] 379.9, found 379.9.

2.3 Synthesis of 6

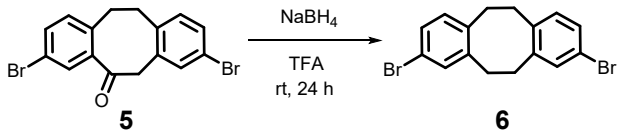

5 **6**

To the solution of $NaBH_4$ (1.50 g, 39.47 mmol) in trifluoroacetic acid (40 mL) was added a solution of **5** (1.00 g, 2.63 mmol) in CH_2Cl_2 dropwise at 0° C. After stirring for 1 d at r.t., another amount of $NaBH_4$ (0.75 g, 19.73 mmol) was added and stirred for 2 h. The quenched reaction was extracted three times with CH_2Cl_2. The combined organic layers were dried over Na_2SO_4 and purified by flash chromatography using PE as eluent to give **6** (0.29 g, yield: 30%). ^{1}H NMR (400 MHz, $CDCl_3$) δ 7.12 (dd, *J* = 6.0, 2.0 Hz, 4H), 6.86–6.79 (m, 2H), 3.02 (d, *J* = 6.0 Hz, 8H). ^{13}C NMR (101 MHz, $CDCl_3$) δ 142.1, 139.0, 132.5, 131.4, 129.2, 119.7, 34.5, 34.2. GC-MS (m/z): calcd. for $C_{21}H_{12}Br_2O_2$ [M^+] 365.9, found 366.0.

2.4 Synthesis of 7

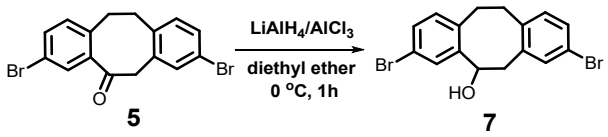

5 **7**

Dry diethyl ether (20 mL) was added in a 100 mL two-necked round-bottom flask equipped with a condenser in the ice bath under N_2. $AlCl_3$ (0.42 g, 3.10 mmol) and $LiAlH_4$ (61 mg, 1.61 mmol) were then added slowly to the ether solution and kept stirring for 20 min. A solution of **5** (0.20 g, 0.5 mmol) in ether (20 mL) was then added dropwise. After stirring for 1 h, ethyl acetate (1 mL) was added dropwise to quench the reaction. The mixture was poured into a saturated NH_4Cl solution (20 mL), and the organic layer was separated and washed with brine (20 mL). The aqueous layer was further extracted with CH_2Cl_2 (20 mL × 3), and the combined organic phase was dried over anhydrous Na_2SO_4. The product was purified via column chromatography on silica gel (CH_2Cl_2/PE=1/3, v/v) to yield product **7** (0.15 g, yield: 75%) as a white powder. ^{1}H NMR (400 MHz, $CDCl_3$) δ 7.40 (d, *J* = 2.0 Hz, 1H), 7.17 (dd, *J* = 8.0, 2.0 Hz, 1H), 7.14–7.08 (m, 2H), 6.80 (q, *J* = 8.0 Hz, 2H), 5.28–5.18 (m, 1H), 3.50 (q, *J* = 8.0 Hz, 1H), 3.31–3.18 (m, 1H), 3.14–2.92 (m, 4H), 2.04 (d, *J* = 3.5 Hz, 1H). ^{13}C NMR (101 MHz,

$CDCl_3$) δ 143.5, 139.4, 138.0, 136.5, 132.8, 131.9, 131.7, 130.7, 129.7, 120.4, 119.8, 77.2, 73.6, 43.5, 34.2, 33.0. GC-MS (m/z): calcd. for $C_{21}H_{12}Br_2O_2$ [M^+] 381.9, found 382.0.

2.5 Synthesis of 8

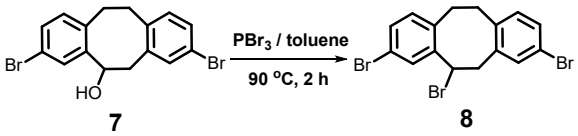

PBr_3 (333 g, 1.23 mmol) was added to a solution of **7** (234 mg, 0.61 mmol) in dry toluene (20 mL). The resulting mixture was heated at 95 °C for 2 h. The reaction mixture was poured into water and extracted with toluene. The organic layer was washed with water, dried over $MgSO_4$, and concentrated under reduced pressure. The residue was purified by column chromatography on silica gel (CH_2Cl_2/PE=1/3, v/v) to yield **8** (0.15 g, yield: 75%) as a white powder. ^{1}H NMR (400 MHz, $CDCl_3$) δ 7.22 (dd, *J* = 8.0, 2.0 Hz, 1H), 7.18–7.08 (m, 3H), 6.90 (d, *J* = 8.0 Hz, 1H), 6.72 (d, *J* = 8.0 Hz, 1H), 5.19 (dd, *J* = 16.0, 12.0 Hz, 1H), 3.86 (dd, *J* = 16.0, 12.0 Hz, 1H), 3.62-3.57 (m, 1H), 3.43-3.36 (m, 2H), 3.06–2.83 (m, 2H).^{13}C NMR (101 MHz, $CDCl_3$) δ 140.0, 138.6, 137.7, 137.6, 133.0, 132.6, 132.5, 132.1, 131.9, 130.5, 120.2, 120.0, 52.4, 43.7, 34.3, 31.8. GC-MS (m/z): calcd. for $C_{21}H_{12}Br_2O_2$ [M^+] 443.9, found 443.9.

2.6 Synthesis of (*Z*)-9

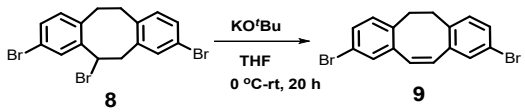

To an ice-cold suspension of KO^{t}Bu (79 mg, 0.70 mmol) in dry THF (3 mL) was added a solution of **8** (100 mg, 0.22 mmol) in THF over 5 min. The reaction mixture was stirred for 20 h at rt., 1.5 mL of H_2O was added and the mixture was poured onto a pad of silica gel wetted with diethyl ether. The pad was rinsed with diethyl ether (8 mL) and the collected organic phase was dried over Na_2SO_4. The solvent was removed under reduced pressure and the crude product was purified by column chromatography on silica gel using PE as eluent. The resulting product was further precipitated from methanol.^{1}H NMR (400 MHz, $CDCl_3$) δ 7.23–7.16 (m, 4H), 7.03–6.95 (m, 2H), 6.70 (s, 2H), 3.11 (s, 4H). ^{13}C NMR (101 MHz, $CDCl_3$) δ 138.5, 138.0, 132.1, 131.5, 131.4, 130.1, 119.2, 34.6. GC-MS (m/z): calcd. for $C_{21}H_{12}Br_2O_2$ [M^+] 363.9, found 364.0.

2.7 Synthesis of 10

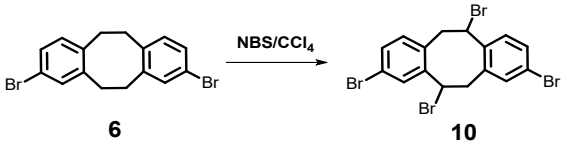

To a solution of **6** (0.12 g, 0.33 mmol) in dry CCl_4 (15 mL) was added NBS (0.17 g, 0.98 mmol) and the resulting reaction mixture was refluxed at 80 °C for 20 h. The hot suspension was filtered through a fritted funnel and the residue was washed with CCl_4 (10 mL). The filtrate was evaporated under reduced pressure. The crude product was purified by column chromatography on silica gel using PE as eluent to give **10** (0.10 g, yield: 60%). ^{1}H NMR (400 MHz, $CDCl_3$) δ 7.29–7.26 (m, 1H), 7.25–7.14 (m, 3H), 6.95 (d, *J* = 8.0 Hz, 1H), 6.85 (d, *J* = 8.0 Hz, 1H), 5.28–5.14 (m, 2H), 4.25–4.10 (m, 2H), 3.65–3.52 (m, 2H). ^{13}C NMR (101 MHz, $CDCl_3$) δ 140.2, 138.0, 137.3, 135.0, 133.8, 133.7, 132.5, 132.4, 132.2, 131.3, 123.1, 121.5, 50.9, 50.5, 42.9, 42.8. GC-MS (m/z): calcd. for $C_{21}H_{12}Br_2O_2$ [M^+] 523.8, found 523.8.

2.8 Synthesis of (5*Z*, 11*Z*)-11

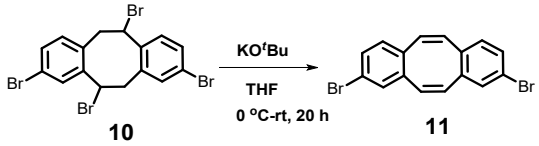

To an ice-cold suspension of KO^{t}Bu (0.76 g, 6.77 mmol) in dry THF (10 mL) was added a solution of **10** (0.44 g, 1.91 mmol) in THF over 5 min. The reaction mixture was stirred for 20 h at r.t. Water (3.0 mL) was added and the mixture was poured onto a pad of silica gel wetted with diethyl ether. The pad was rinsed with diethyl ether (10 mL) and the collected organic phase was dried over Na_2SO_4. The solvent was removed under reduced pressure and the crude product was purified by column chromatography on silica using PE as eluent. Crystallization was performed in methanol to give product **11** (0.24 g, yield: 80%).^{1}H NMR (400 MHz, $CDCl_3$) δ 7.28 (dd, *J* = 8.0, 2.0 Hz, 2H), 7.21 (d, *J* = 2.0 Hz, 2H), 6.91 (d, *J* = 8.0 Hz, 2H), 6.68 (d, *J* = 8.0 Hz, 4H). ^{13}C NMR (101 MHz, $CDCl_3$) δ 138.7, 135.7, 132.9, 132.8, 131.7, 130.6, 130.2, 121.0. GC-MS (m/z): calcd. for $C_{21}H_{12}Br_2O_2$ [M^+] 361.9, found 362.0.

2.9 Synthesis of 12

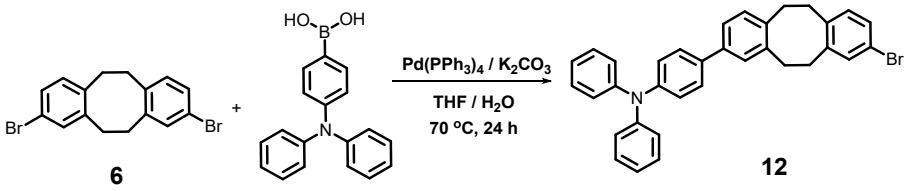

A mixture of **6** (0.20 g, 0.55 mmol), (4-(diphenylamino)phenyl)boronic acid (166 mg, 0.57 mmol), K_2CO_3 (0.23 g, 1.66 mmol) and $Pd(PPh_3)_4$ (32 mg, 27 μmol) in THF (10 mL) and deionized water (2 mL) was refluxed under N_2 for 24 h. After the mixture was cooled down, deionized water (10 mL) was added to the resulting solution and the mixture was extracted with CH_2Cl_2 three times. The organic phase was dried over Na_2SO_4 and was further purified by column chromatography on silica gel using

CH_2Cl_2/PE (1/8, v/v) as eluent to give **12** as a white solid (0.12 g, yield: 40%). ^{1}H NMR (400 MHz, $CDCl_3$) δ 7.41 (d, J = 8.0 Hz, 2H), 7.30–7.18 (m, 6H), 7.15–7.06 (m, 8H), 7.05–6.96 (m, 3H), 6.86 (d, J = 8.0 Hz, 1H), 3.15–3.01 (m, 8H). ^{13}C NMR (101 MHz, $CDCl_3$) δ 147.7, 146.9, 142.7, 140.3, 139.5, 138.8, 138.5, 135.0, 132.5, 131.4, 130.2, 129.2, 129.1, 128.1, 127.5, 124.4, 124.3, 124.1, 122.8, 119.6, 35.0, 34.9, 34.5. ESI-HRMS (m/z): calcd. for $C_{34}H_{28}BrN$ $[M+H]^+$ 530.1483, found 530.1494.

2.10 Synthesis of M1

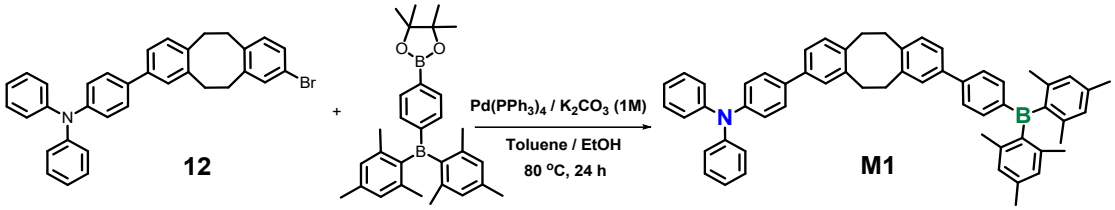

The mixture of **12** (0.10 g, 0.19 mmol), 2-(4-(dimesitylboryl)phenyl)-4,4,5,5-tetramethyl-1,3,2-dioxaborolane (0.11 g, 0.24 mmol), $Pd(PPh_3)_4$ (10 mg, 9 μmol), toluene (6 mL), ethanol (2 mL) and 1 M K_2CO_3 aqueous solution (1 mL) in the round-bottom flask were heated to 80 ˚C, and stirred under an argon atmosphere for 8 h. The mixture was then cooled to r.t. and poured into H_2O (100 mL). After extraction with CH_2Cl_2, the organic phase was dried over Na_2SO_4. Purification by column chromatography on silica using CH_2Cl_2/ petroleum ether (1:6, v/v) as eluent yielded **M1** (44 mg, yield: 30%). ^{1}H NMR (400 MHz, $CDCl_3$) δ 7.56–7.48 (m, 4H), 7.42–7.37 (m, 2H), 7.32 (d, J = 4.0 Hz, 2H), 7.23–7.18 (m, 6H), 7.12–7.05 (m, 8H), 7.03–6.97 (m, 2H), 6.82 (s, 4H), 3.15 (d, J = 12.0 Hz, 8H), 2.31 (s, 6H), 2.01 (s, 12H). ^{13}C NMR (101 MHz, $CDCl_3$) δ 147.7, 146.8, 144.2, 140.8, 138.5, 138.4, 138.4, 137.1, 135.1, 130.3, 130.2, 129.2, 128.6, 128.1, 127.5, 126.3, 124.9, 124.3, 124.2, 124.1, 122.8, 35.5, 35.0, 34.9, 23.5, 21.2. ^{11}B NMR (225 MHz, $CDCl_3$) δ 75 ppm. ESI-HRMS (m/z): calcd. for $C_{58}H_{54}BN$ $[M+H]^+$ 776.4428, found 776.4414.

2.11 Synthesis of (*Z*)-13

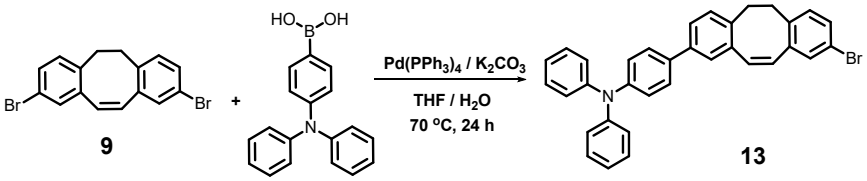

A mixture of **9** (0.15 g, 0.41 mmol), (4-(diphenylamino)phenyl)boronic acid (0.12 g, 0.42 mmol), K_2CO_3 (0.25 g, 1.80 mmol) and $Pd(PPh_3)_4$ (24 mg, 21 μmol) in THF (20 mL) and deionized water (4 mL) was refluxed at 70 °C under N_2 for 24 h. After the mixture was cooled down, the reaction was quenched with water (10 mL) and was then extracted with CH_2Cl_2 three times. The organic phase was dried over anhydrous $MgSO_4$, and the crude product was purified by column chromatography on silica gel

using CH_2Cl_2/ petroleum ether (1:8, v/v) as an eluent to give **13** as a white solid (76 mg, yield: 35%). ^{1}H NMR (400 MHz, $CDCl_3$) δ 7.43–7.37 (m, 2H), 7.33–7.15 (m, 9H), 7.14–7.06 (m, 6H), 7.05–6.98 (m, 3H), 6.84 (d, J = 12.4 Hz, 1H), 6.69 (d, J = 12.4 Hz, 1H), 3.25–3.10 (m, 4H). ^{13}C NMR (101 MHz, $CDCl_3$) δ 147.7, 147.0, 138.9, 138.6, 137.9, 137.5, 136.6, 134.6, 132.8, 132.1, 131.4, 130.6, 130.2, 129.9, 129.2, 128.0, 127.5, 125.4, 124.3, 124.0, 122.9, 119.0, 35.1, 34.7. ESI-HRMS (m/z): calcd. for $C_{34}H_{26}BrN$ $[M+H]^+$ 528.1327, found 528.1324.

2.12 Synthesis of M2

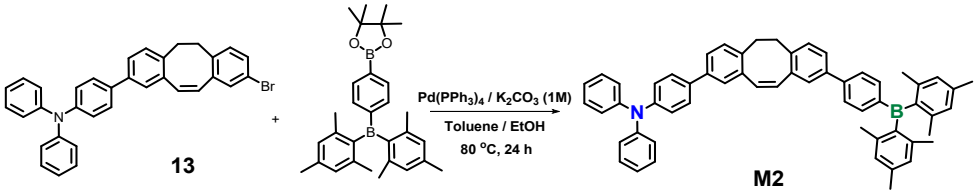

The mixture of **13** (0.10 g, 0.19 mmol), 2-(4-(dimesitylboryl)phenyl)-4,4,5,5-tetramethyl-1,3,2-dioxaborolane (0.11 g, 0.24 mmol), $Pd(PPh_3)_4$ (10 mg, 8.65 mmol), toluene (6 mL), ethanol (2 mL) and 1 M K_2CO_3 aqueous solution (1 mL) in the round-bottom flask were heated to 80 ˚C, and stirred under an argon atmosphere for 8 h. The mixture was then cooled to room temperature and poured into water (100 mL). After extraction with CH_2Cl_2, the organic phase was dried over Na_2SO_4. Purification by column chromatography on silica gel using CH_2Cl_2/ petroleum ether (1:10, v/v) as eluent yielded **M2** (59 mg, 40%). Crystallization was performed in CH_2Cl_2/hexane. ^{1}H NMR (400 MHz, $CDCl_3$) δ 7.56–7.48 (m, 4H), 7.42–7.36 (m, 4H), 7.32–7.28 (m, 2H), 7.25–7.18 (m, 6H), 7.13–7.05 (m, 6H), 7.04–6.97 (m, 2H), 6.84 (s, 2H), 6.82 (s, 4H), 3.26 (s, 4H), 2.31 (s, 6H), 2.01 (s, 12H).^{13}C NMR (101 MHz, $CDCl_3$) δ 147.7, 147.0, 143.9, 140.8, 139.3, 138.6, 138.0, 137.8, 137.2, 137.0, 136.9, 134.8, 131.9, 131.5, 130.5, 128.6, 128.2, 127.6, 126.3, 125.7, 125.3, 124.3, 124.0, 122.8, 35.2, 23.5, 21.2. ^{11}B NMR (225 MHz, $CDCl_3$) δ 75 ppm. ESI-HRMS (m/z): calcd. for $C_{58}H_{52}BN$ [M] 773.4193, found 773,4223.

2.13 Synthesis of (5*Z*, 11*Z*)-14

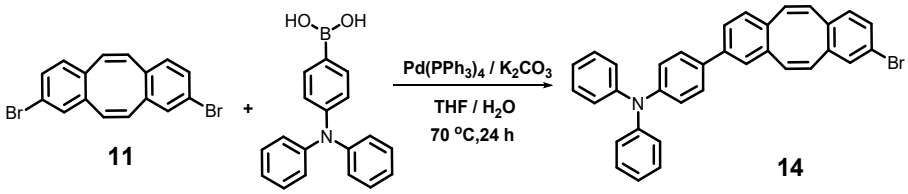

A mixture of **11** (0.17 g, 0.47 mmol), (4-(diphenylamino)phenyl)boronic acid (136 mg, 0.47 mmol), K_2CO_3 (0.26 g, 1.88 mmol) and $Pd(PPh_3)_4$ (27 mg, 23.4 μmol) in THF (15 mL) and deionized water (2 mL) was refluxed under N_2 for 24 h. After the mixture was cooled down, 10 mL of deionized water was added to the resulting solution and the

mixture was extracted with CH_2Cl_2 three times. The organic phase was dried over anhydrous $MgSO_4$, and the residue was purified by column chromatography on silica gel using CH_2Cl_2/ petroleum ether (1:8, v/v) as eluent to give **14** as a white solid (99 mg, yield: 40%). ^{1}H NMR (400 MHz, $CDCl_3$) δ 7.44–7.34 (m, 3H), 7.30–7.20 (m, 7H), 7.15–7.06 (m, 7H), 7.05–6.99 (m, 2H), 6.93 (d, *J* = 8.0 Hz, 1H), 6.80 (t, *J* = 12.4 Hz, 2H), 6.73–6.63 (m, 2H). ^{13}C NMR (101 MHz, $CDCl_3$) δ 147.6, 147.3, 139.4, 139.2, 137.0, 136.1, 135.2, 134.3, 134.2, 133.7, 132.2, 132.0, 131.8, 130.7, 130.0, 129.6, 127.6, 127.2, 125.3, 124.4, 123.8, 123.0, 120.8. ESI-HRMS (m/z): calcd. for $C_{34}H_{24}BrN$ $[M+H]^+$ 526.1170, found 526.1175.

2.14 Synthesis of (5*Z*, 11*Z*)-M3

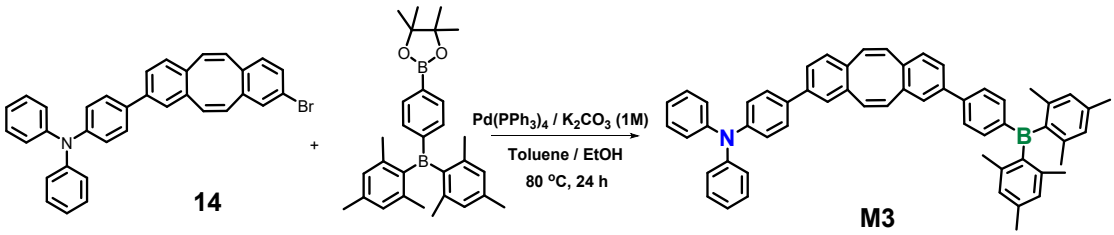

The mixture of **14** (0.10 g, 1.90 mmol), 2-(4-(dimesitylboryl)phenyl)-4,4,5,5-tetramethyl-1,3,2-dioxaborolane (0.10 g, 2.28 mmol), $Pd(PPh_3)_4$ (11 mg, 9.5 μmol), toluene (6 mL), ethanol (2 mL) and 1 M K_2CO_3 aqueous solution (1 mL) in the round-bottom flask were heated to 80 ˚C, and stirred under an argon atmosphere for 8 h. The mixture was then cooled to r.t. and poured into water (100 mL). After extraction with CH_2Cl_2, the organic phase was dried over Na_2SO_4. Purification by column chromatography on silica gel using CH_2Cl_2/ petroleum ether (1:6, v/v) as eluent yielded **M3** (44 mg, yield: 30%).^{1}H NMR (400 MHz, $CDCl_3$) δ 7.57–7.49 (m, 4H), 7.46 (dd, *J* = 8.0, 2.0 Hz, 1H), 7.43–7.34 (m, 4H), 7.30–7.21 (m, 5H), 7.16–7.06 (m, 8H), 7.0 –6.98 (m, 2H), 6.82 (d, *J* = 6.4 Hz, 6H), 6.80 (s, 2H), 2.31 (s, 6H), 2.01 (s, 12H).^{13}C NMR (101 MHz, $CDCl_3$) δ 147.7, 147.2, 143.6, 139.3, 139.2, 138.6, 137.6, 137.4, 137.0, 136.7, 135.5, 134.3, 133.6, 133.4, 133.3, 133.0, 129.8, 129.7, 129.3, 128.2, 127.6, 127.3, 126.3, 125.7, 125.2, 124.4, 123.8, 122.9, 53.4, 23.5, 21.2. ^{11}B NMR (225 MHz, $CDCl_3$) δ 75 ppm. ESI-HRMS (m/z): calcd. for $C_{58}H_{52}BN$ $[M+H]^+$ 772.4115, found 772.4110.

Reference:

[1] P. Mücke, M. Zabel, R. Edge, D. Collison, S. Clément, S. Záliš and R. F. Winter. *Journal of Organometallic Chemistry*, 2011, 3186−3197.

[2] (a) C. Lee, W. Yang, R. G. Parr, *Phys. Rev. B,* **1988**, *37*, 785-789. (b) A. D. Becke, *J. Chem. Phys.* **1993**, *98*, 1372−1377. (c) A. D. Becke, *J. Chem. Phys.* **1993**, *98*, 5648−5652.

3. Characterization by NMR and HRMS Spectroscopy

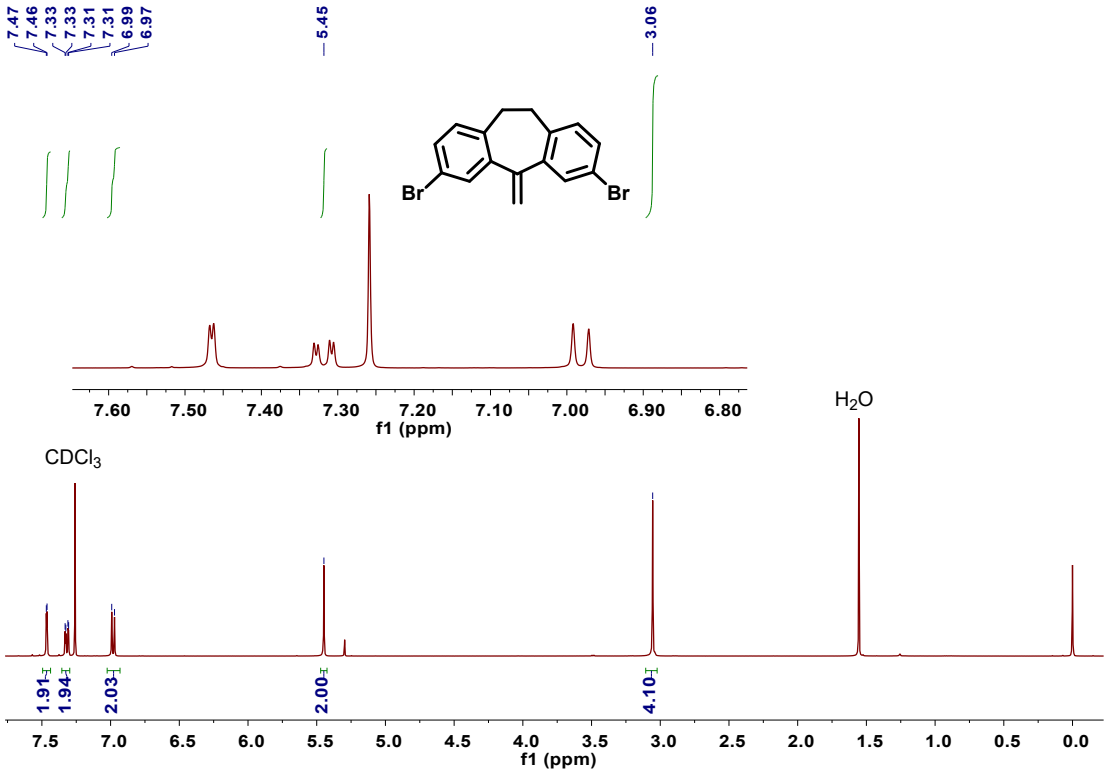

Figure S1. ^{1}H NMR (400 MHz, $CDCl_3$) spectrum of **4**.

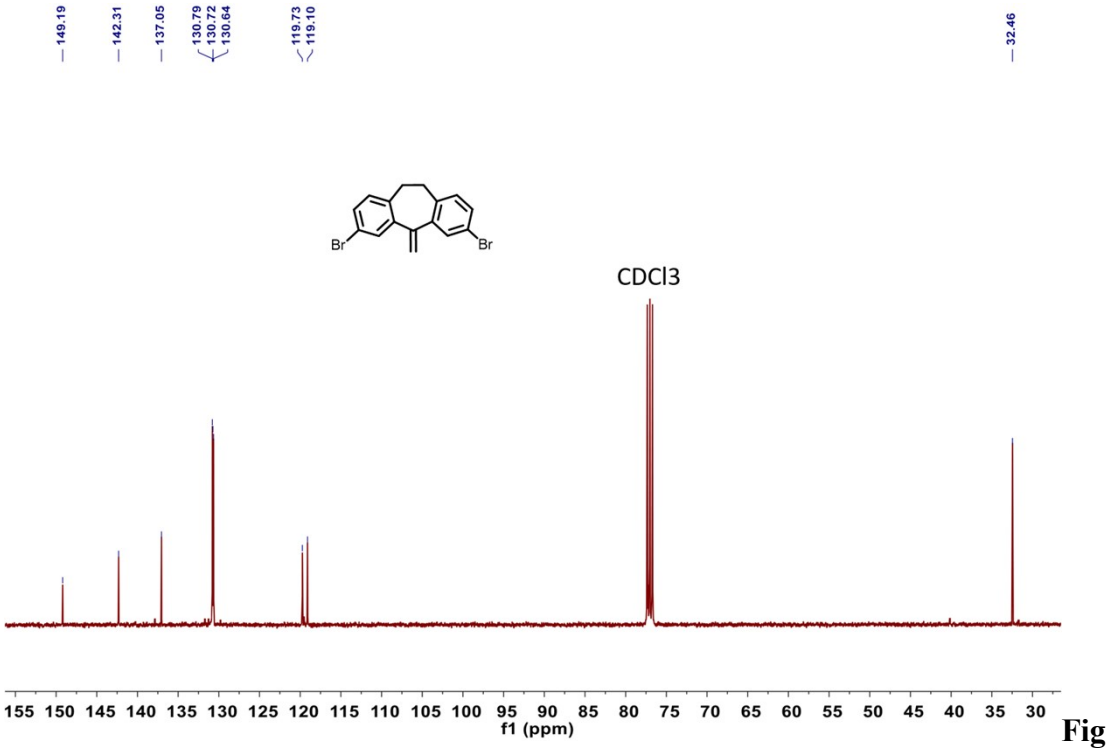

Figure S2. ^{13}C NMR (101 MHz, $CDCl_3$) spectrum of **4**.

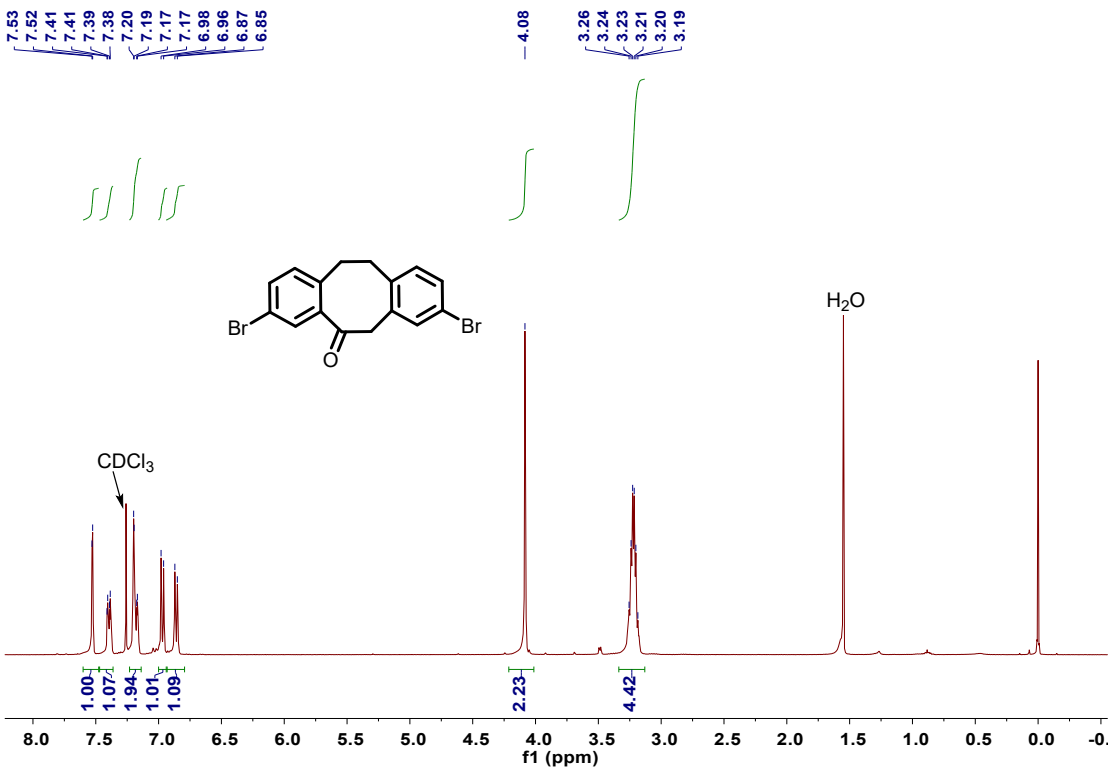

Figure S3. ^{1}H NMR (400 MHz, $CDCl_3$) spectrum of **5**.

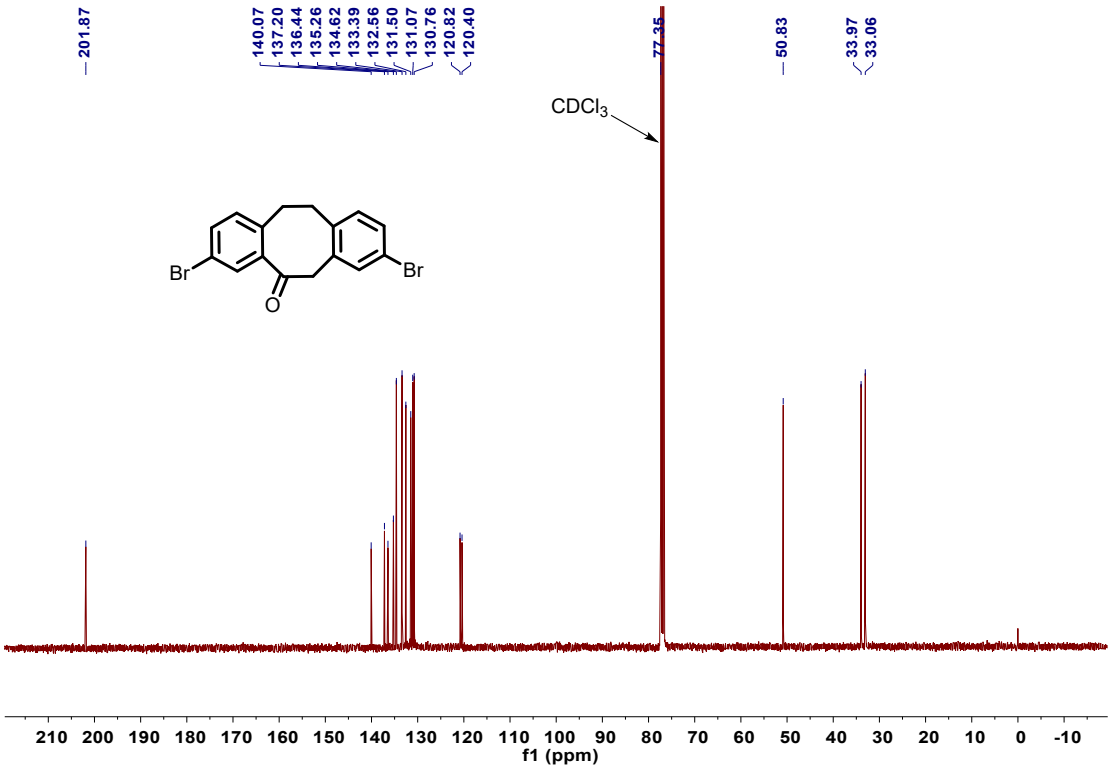

Figure S4. ^{13}C NMR (101 MHz, $CDCl_3$) spectrum of **5**.

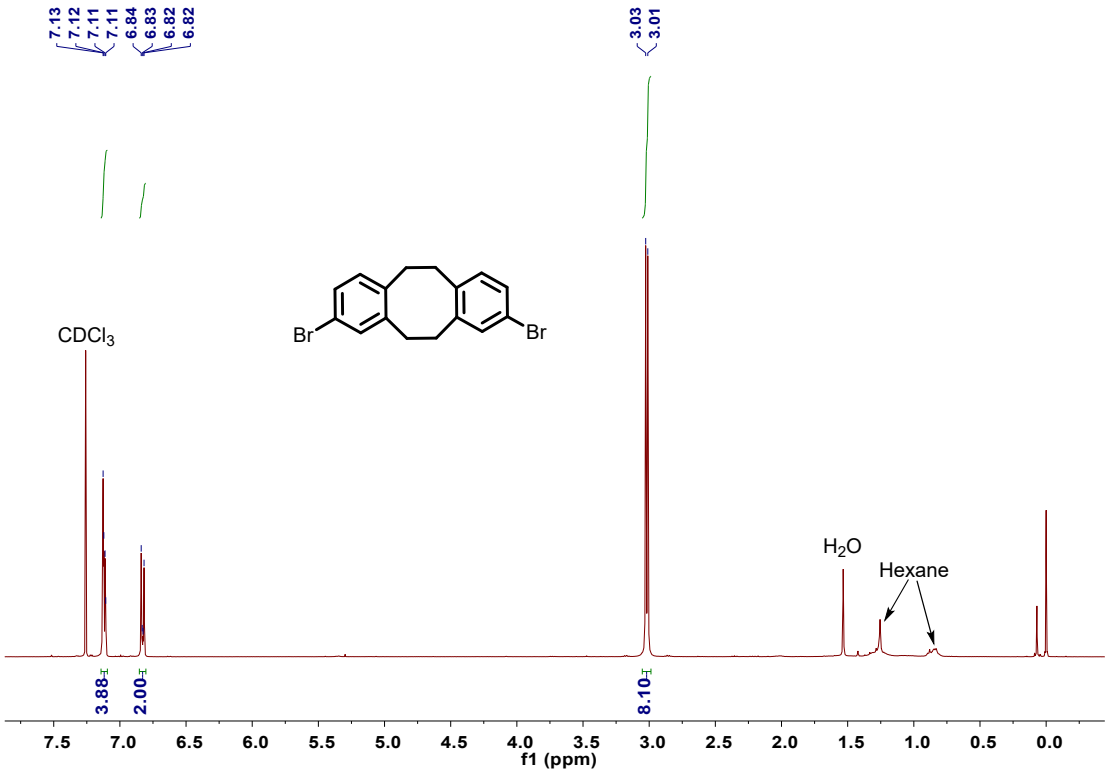

Figure S5. ^{1}H NMR (400 MHz, $CDCl_3$) spectrum of **6**.

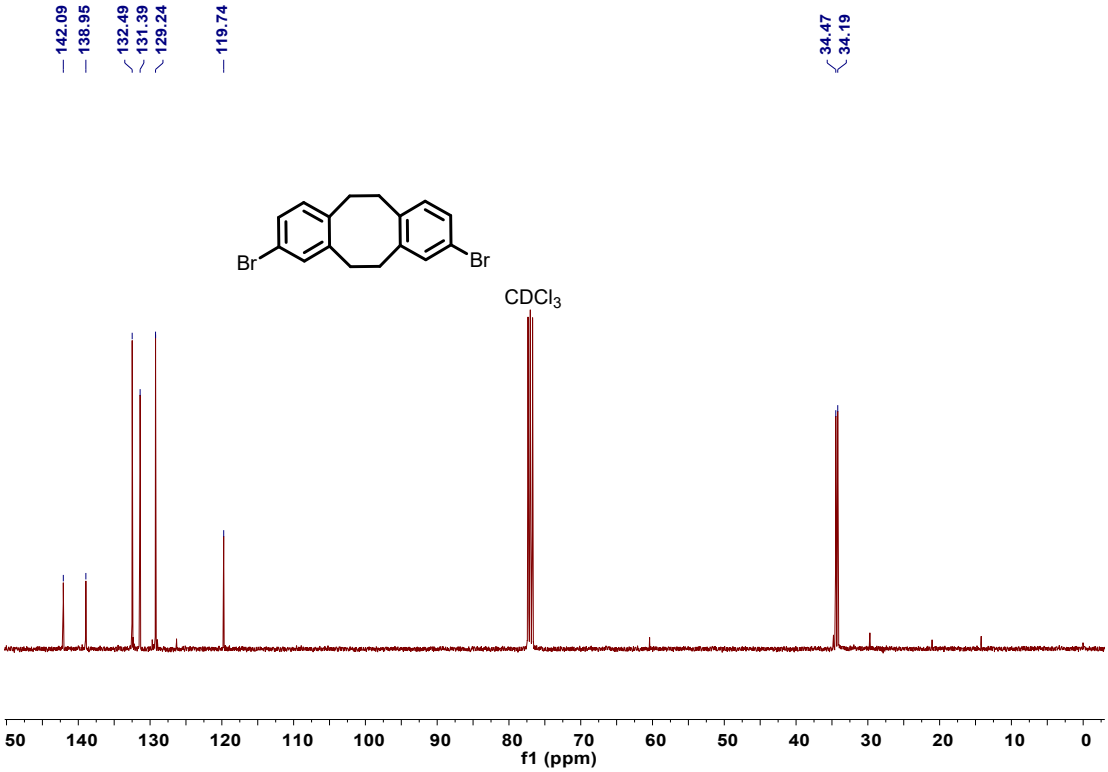

Figure S6. ^{13}C NMR (101 MHz, $CDCl_3$) spectrum of **6**.

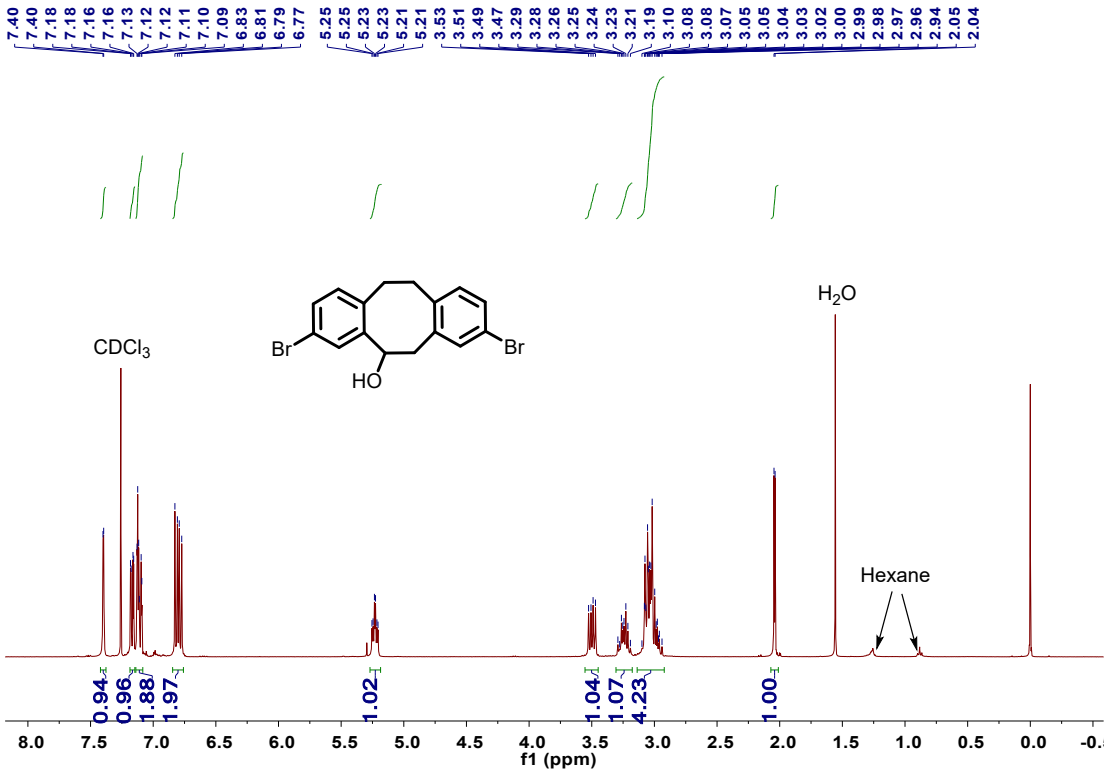

Figure S7. ^{1}H NMR (400 MHz, $CDCl_3$) spectrum of **7**.

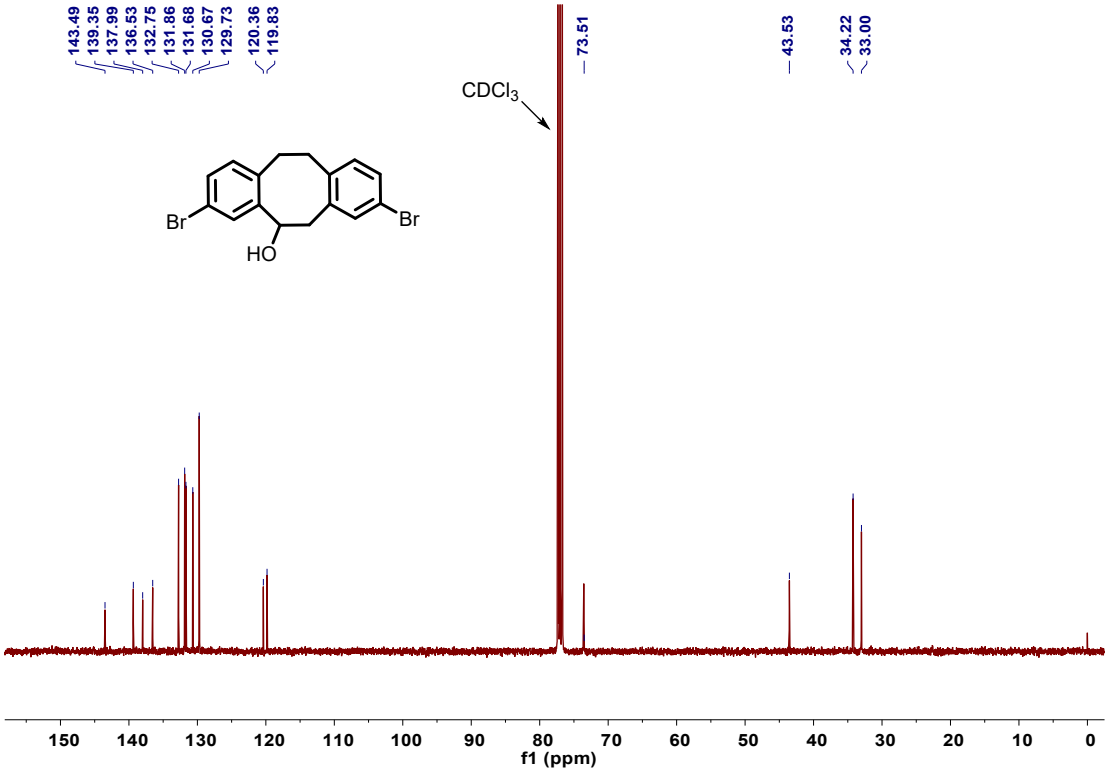

Figure S8. ^{13}C NMR (101 MHz, $CDCl_3$) spectrum of **7**.

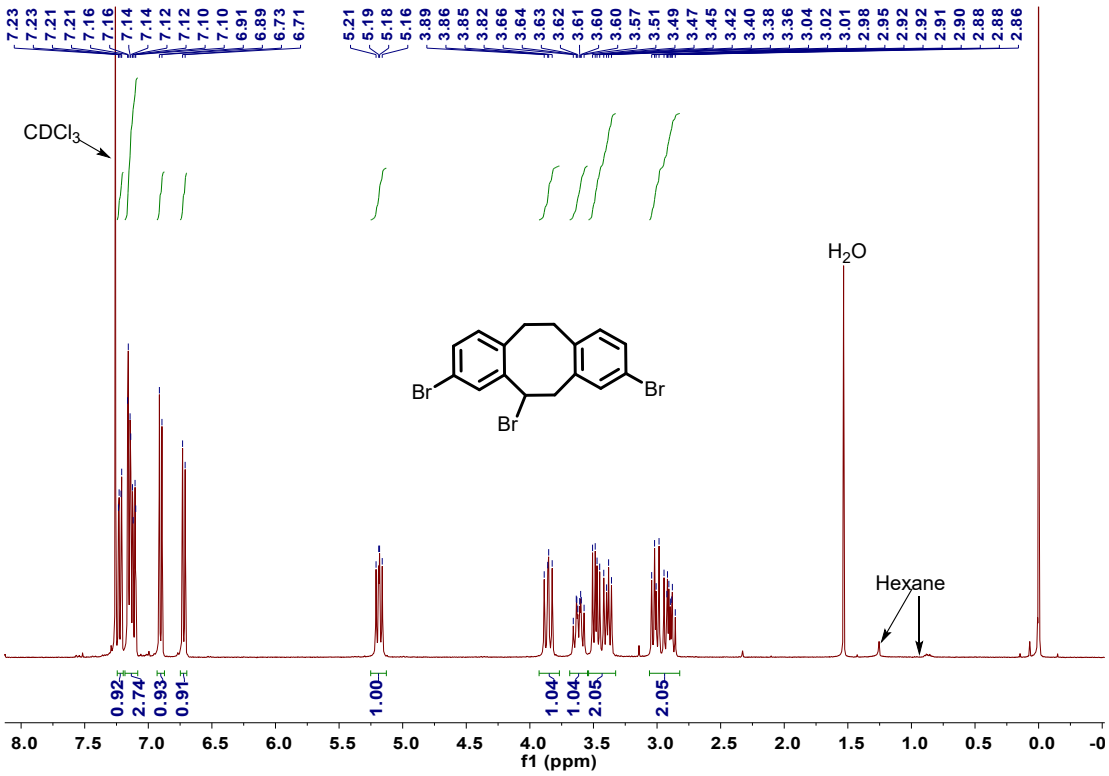

Figure S9. ^{1}H NMR (400 MHz, $CDCl_3$) spectrum of **8**.

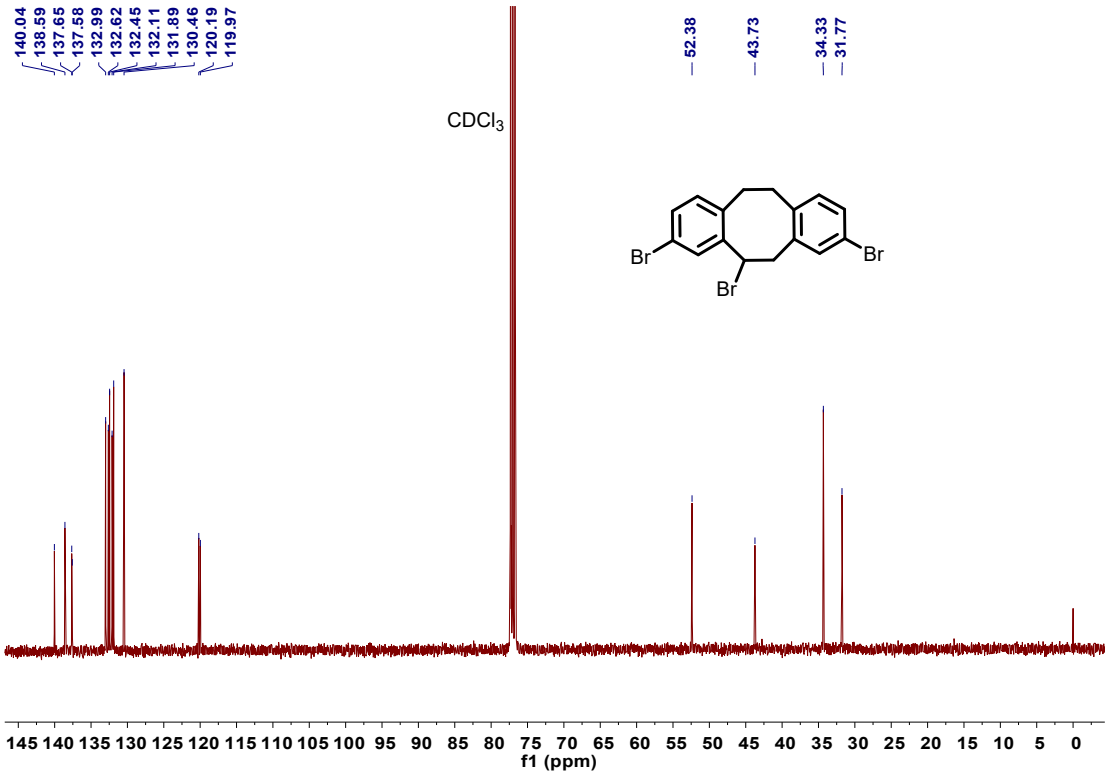

Figure S10. ^{13}C NMR (101 MHz, $CDCl_3$) spectrum of **8**.

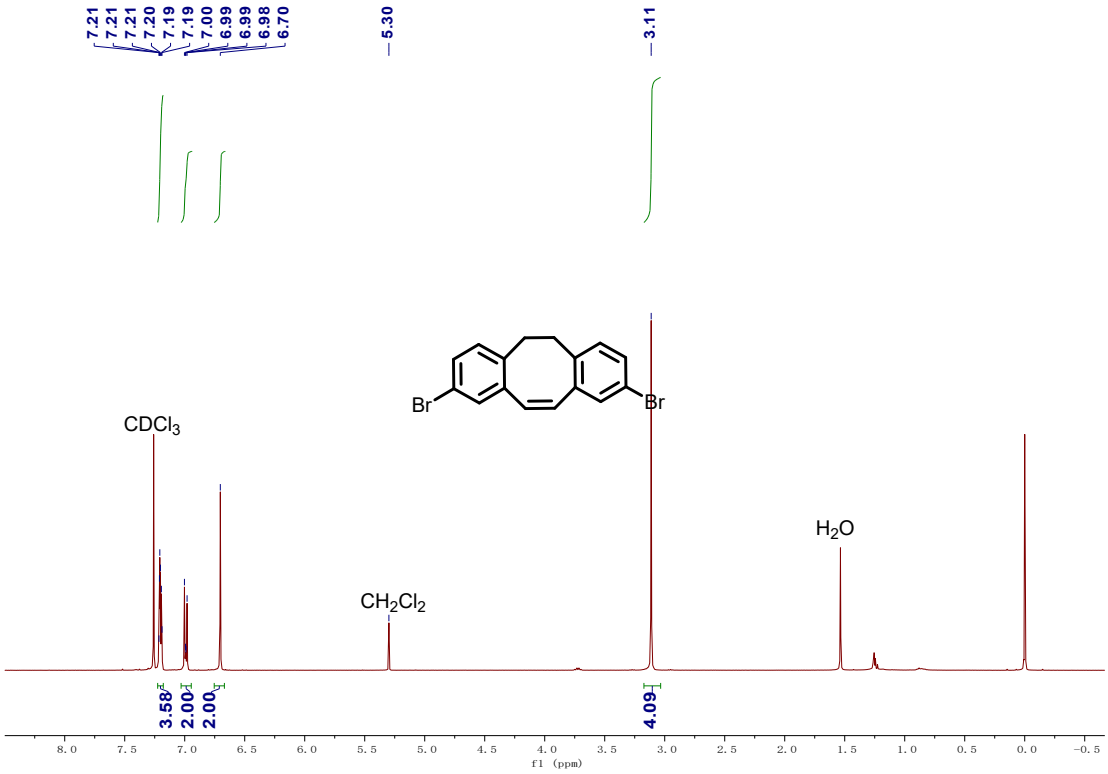

Figure S11. ^{1}H NMR (400 MHz, $CDCl_3$) spectrum of **9**.

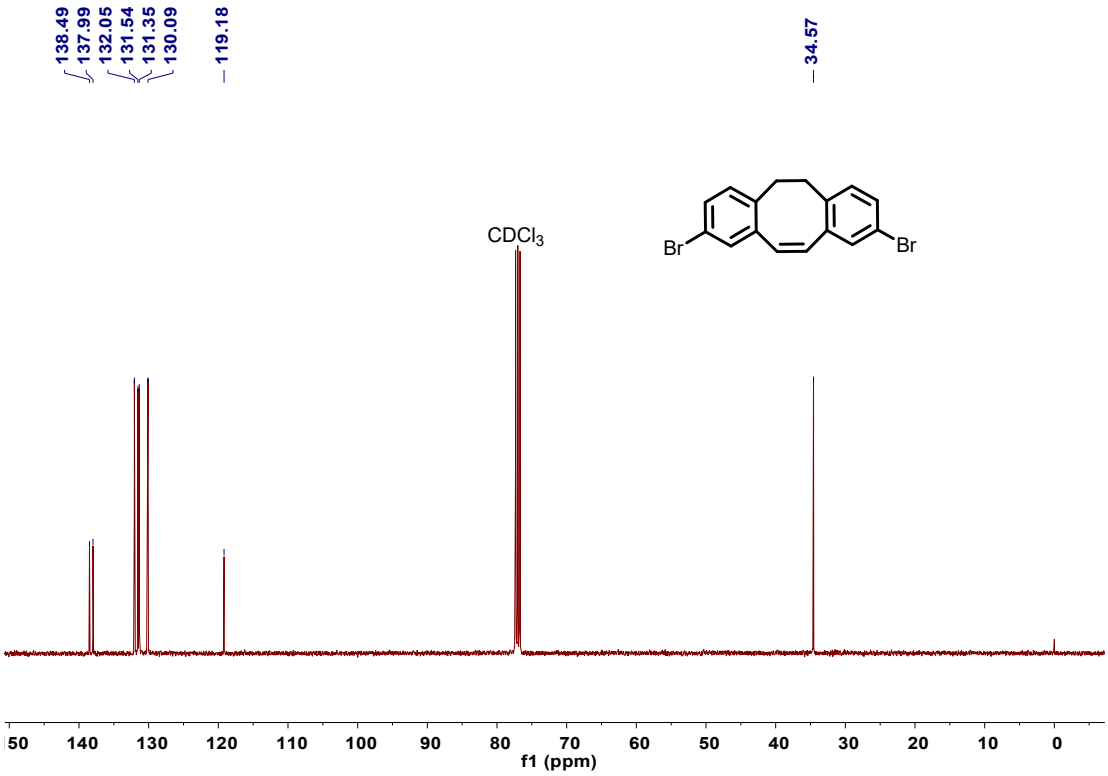

Figure S12. ^{13}C NMR (101 MHz, $CDCl_3$) spectrum of **9**.

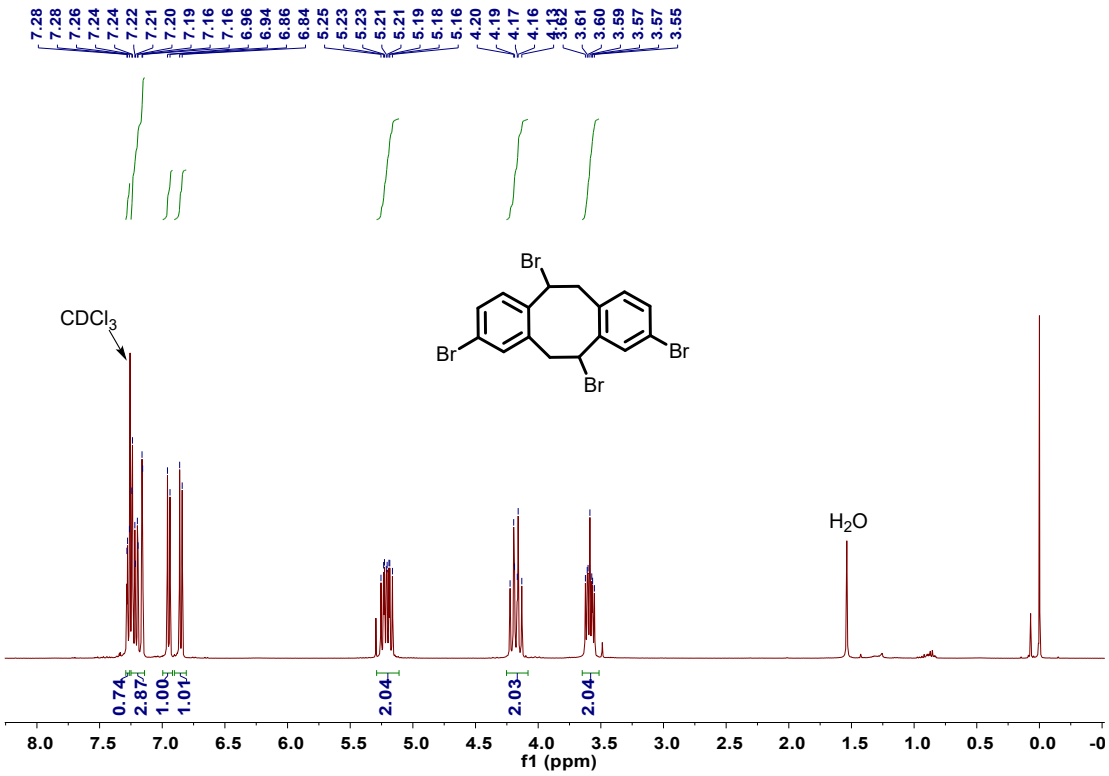

Figure S13. ^{1}H NMR (400 MHz, $CDCl_3$) spectrum of **10**.

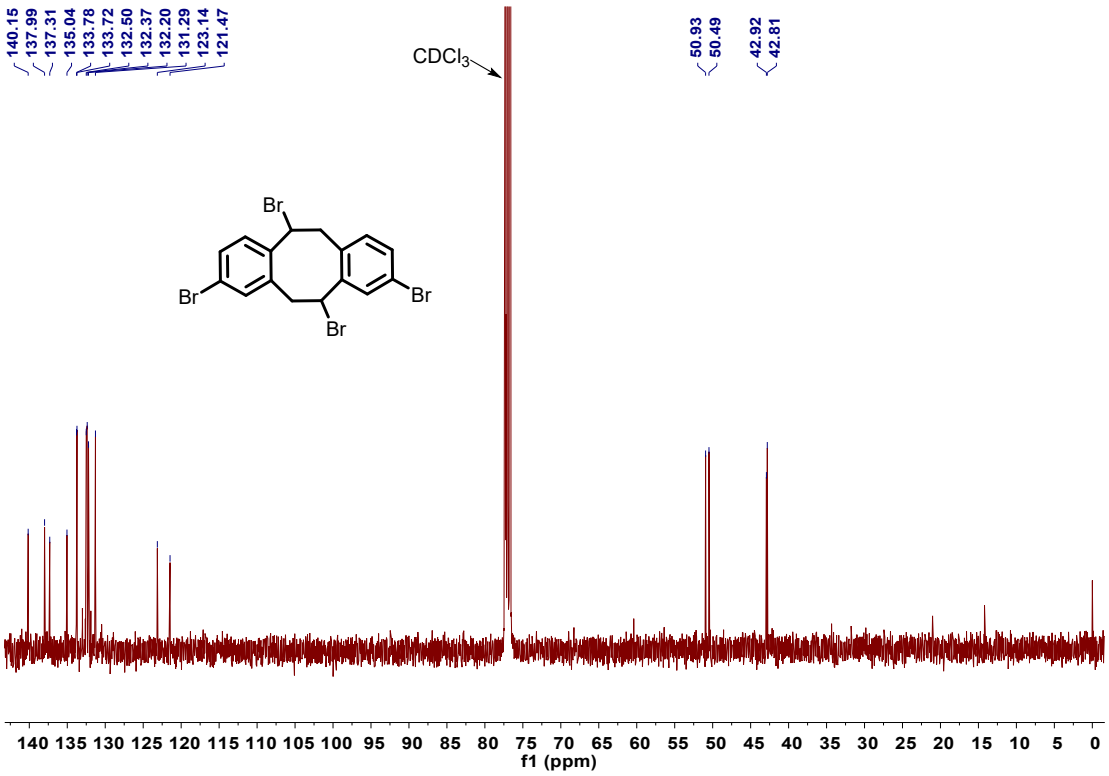

Figure S14. ^{13}C NMR (101 MHz, $CDCl_3$) spectrum of **10**.

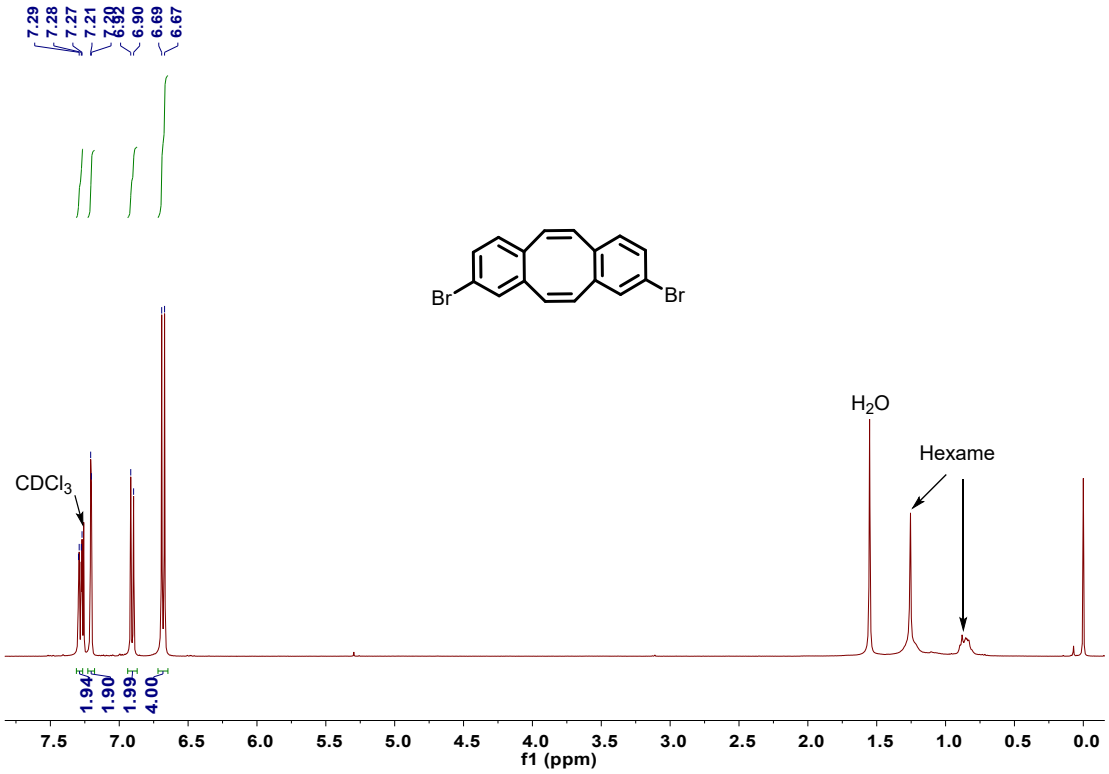

Figure S15. ^{1}H NMR (400 MHz, $CDCl_3$) spectrum of **11**.

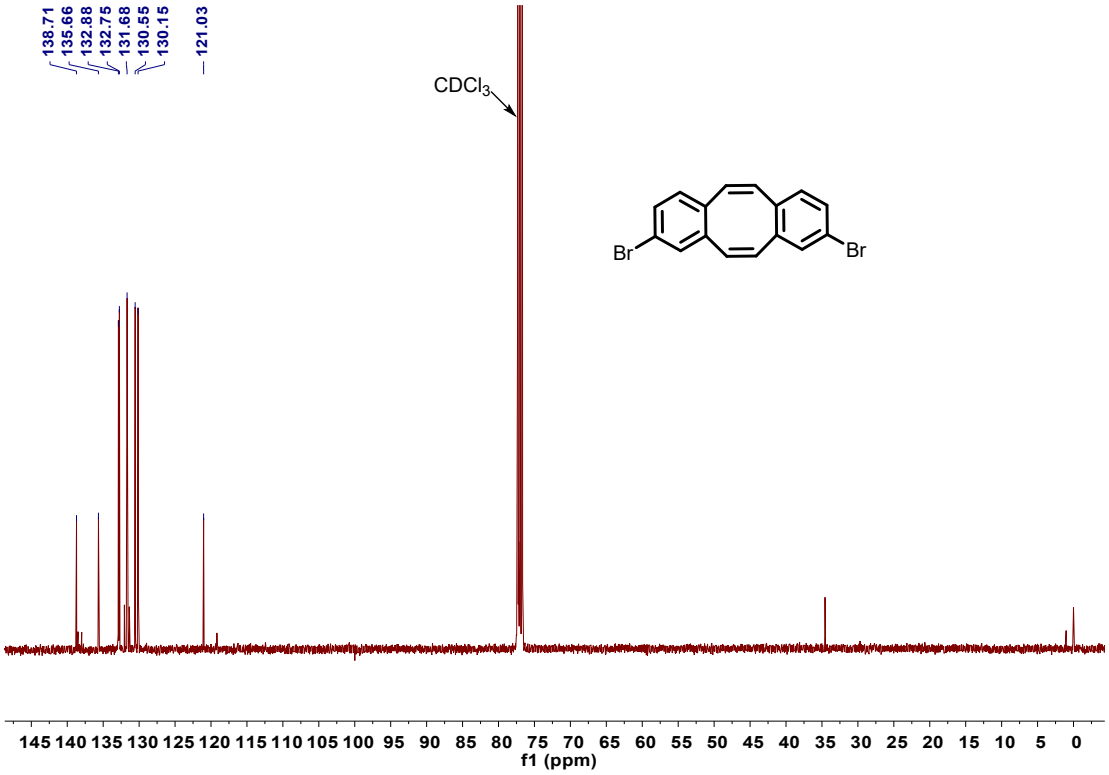

Figure S16. ^{13}C NMR (101 MHz, $CDCl_3$) spectrum of **11**.

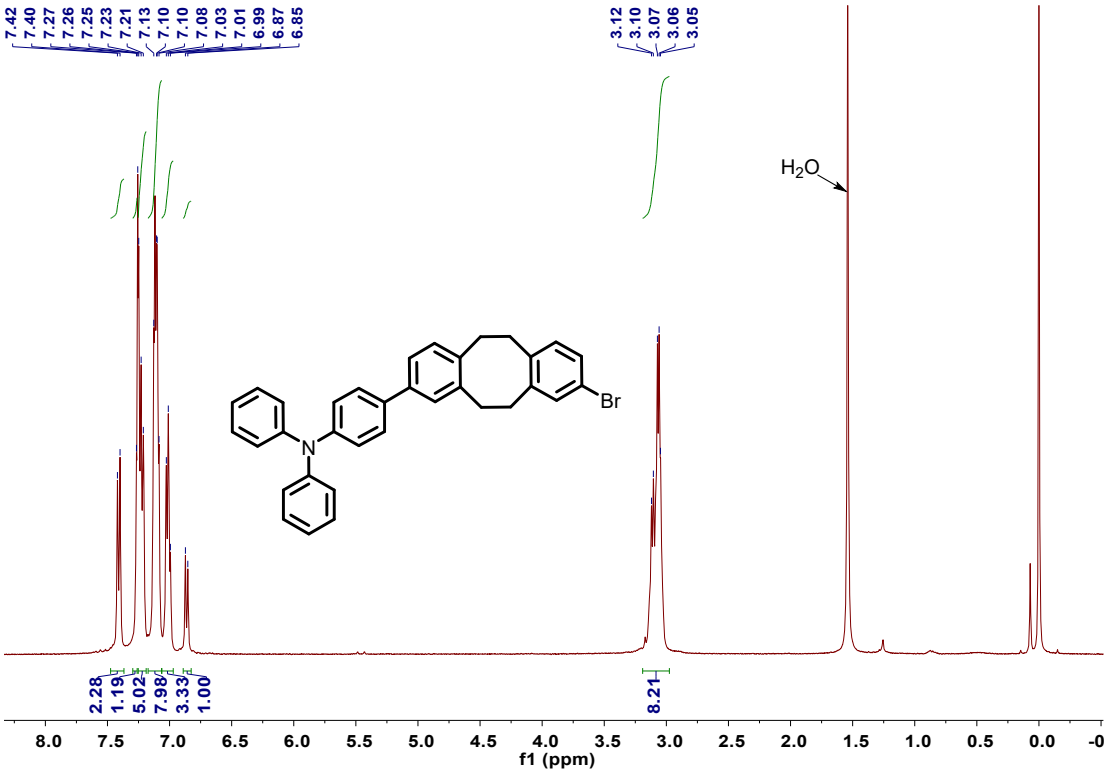

Figure S17. ^{1}H NMR (400 MHz, $CDCl_3$) spectrum of **12**.

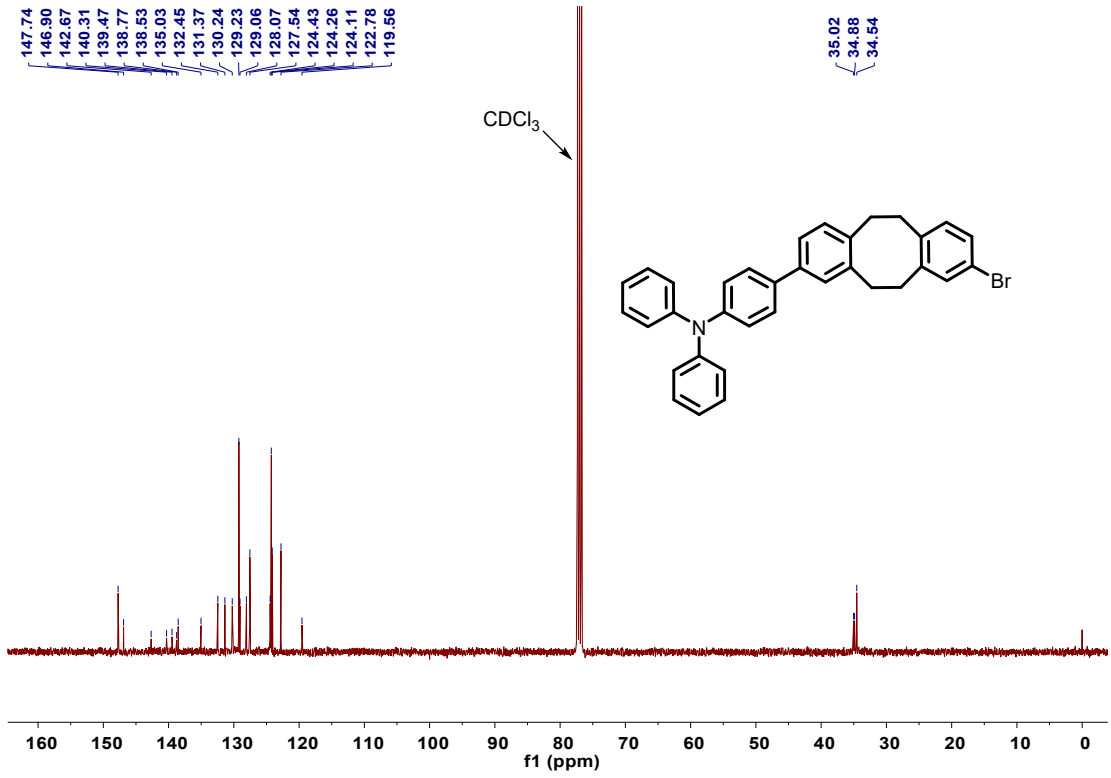

Figure S18. ^{13}C NMR (101 MHz, $CDCl_3$) spectrum of **12**.

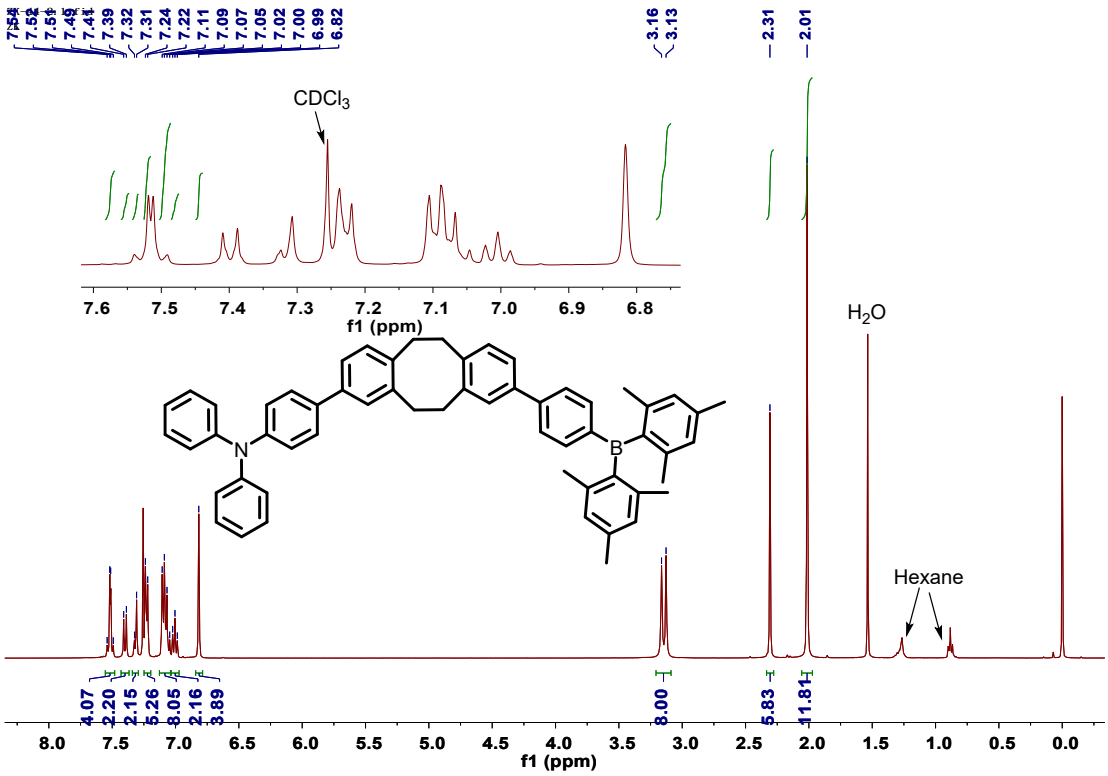

Figure S19. ^{1}H NMR (400 MHz, $CDCl_3$) spectrum of **M1**.

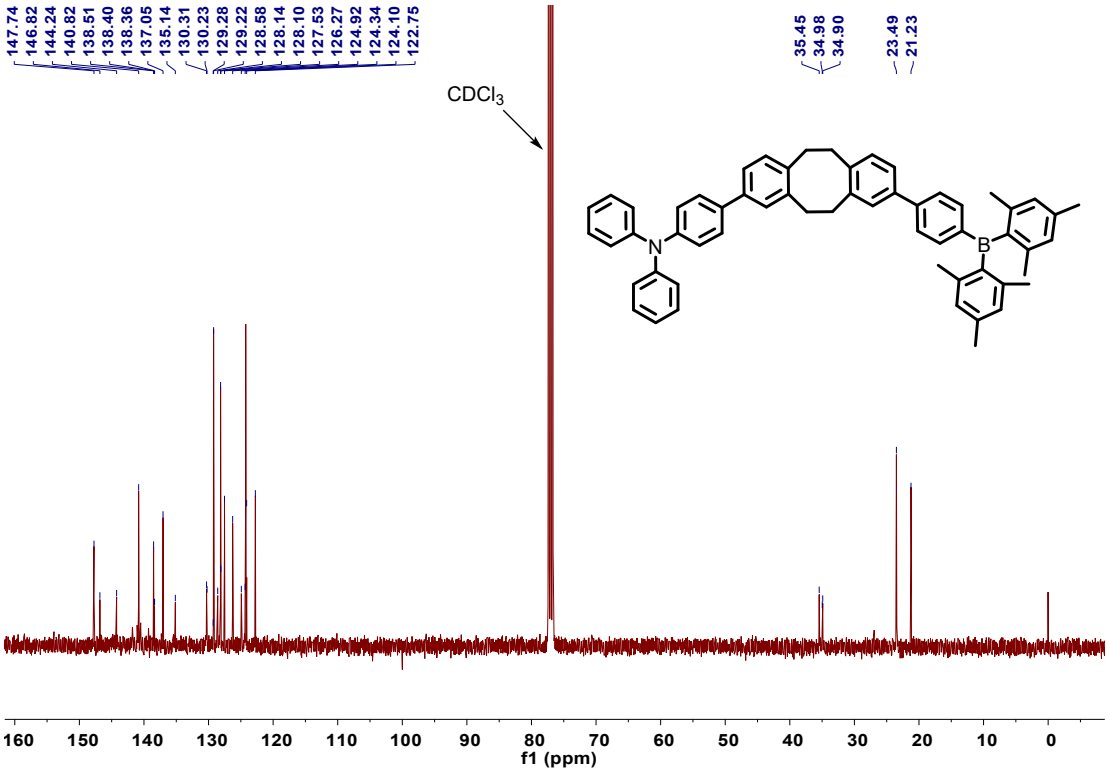

Figure S20. ^{13}C NMR (101 MHz, $CDCl_3$) spectrum of **M1**.

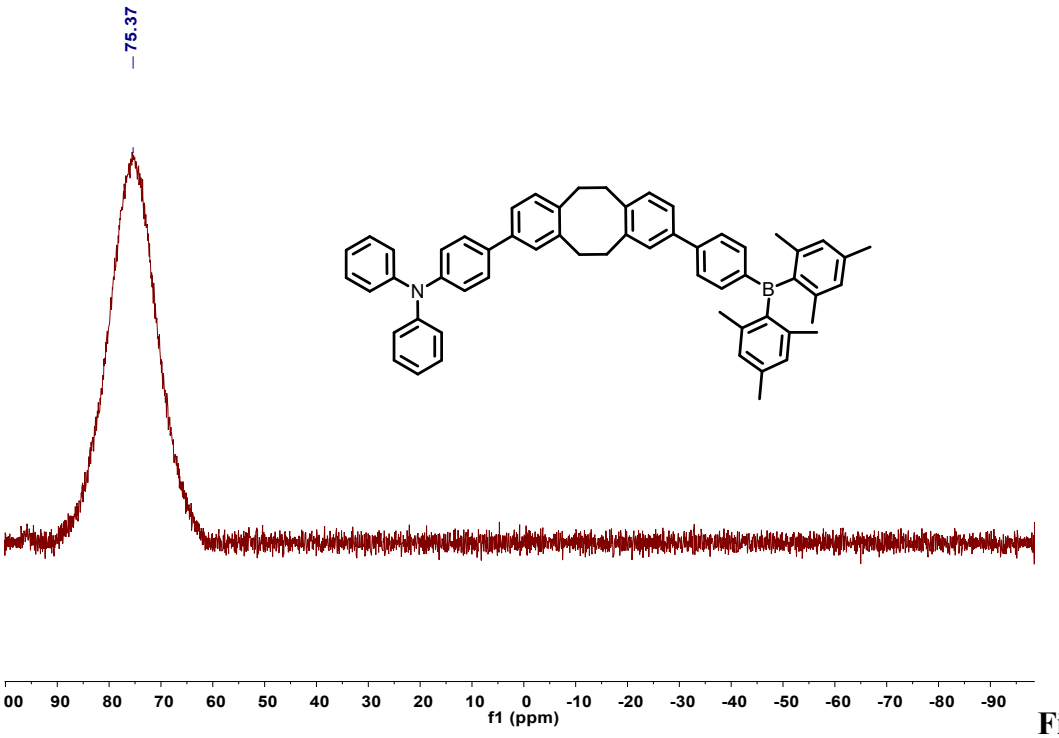

Figure S21.^{11}B NMR (225 MHz, C_6D_6) spectrum of **M1**.

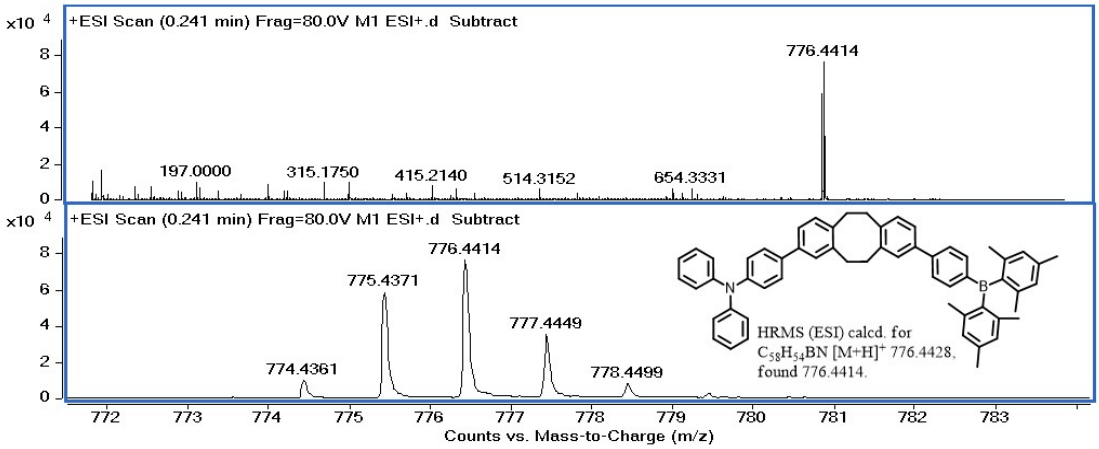

Figure S22. HRMS spectrum for **M1**.

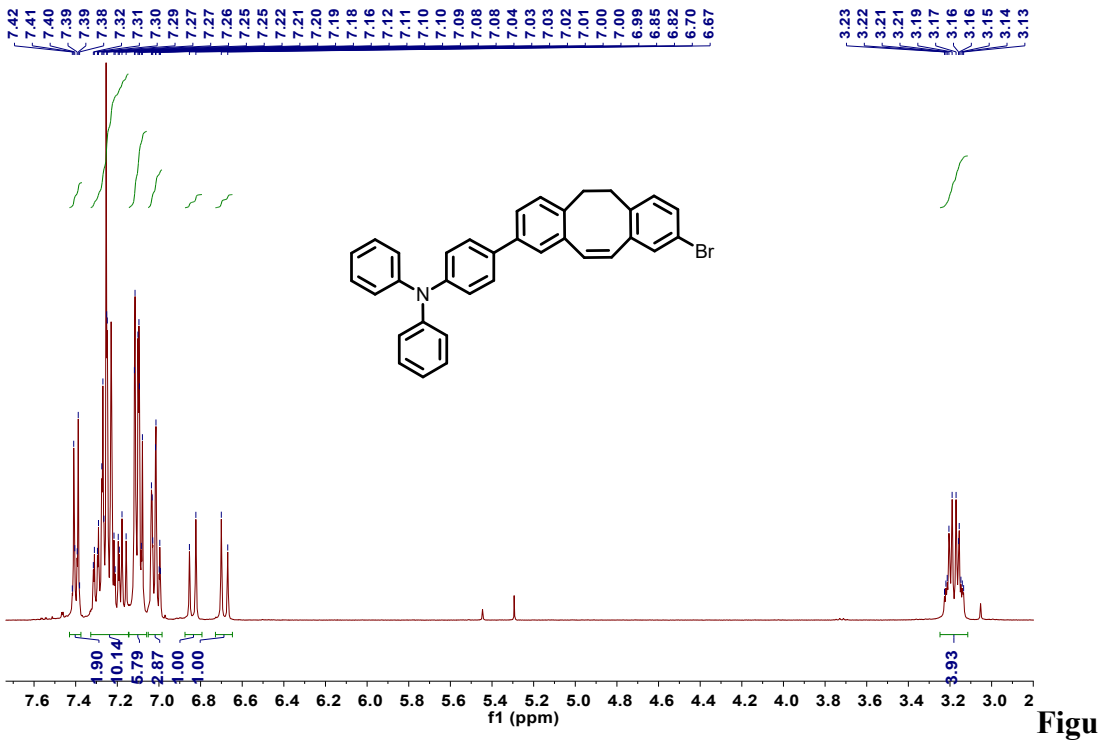

Figure S23. ^{1}H NMR (400 MHz, $CDCl_3$) spectrum of **13**.

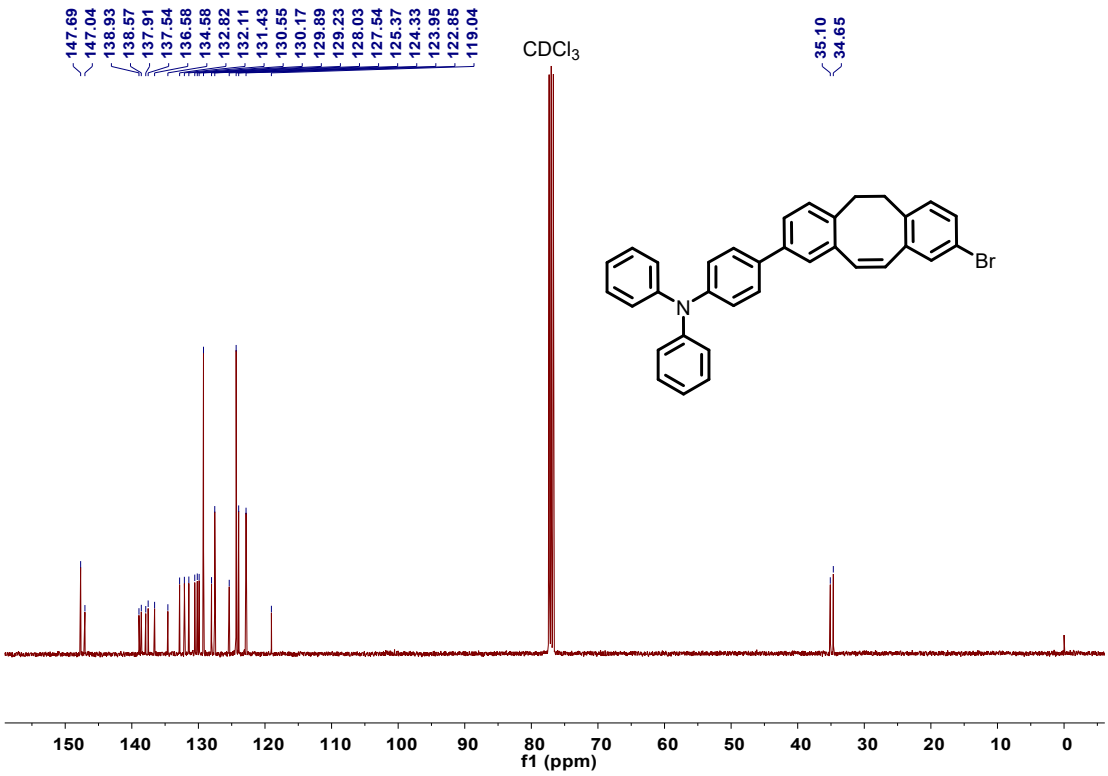

Figure S24. ^{13}C NMR (101 MHz, $CDCl_3$) spectrum of **13**.

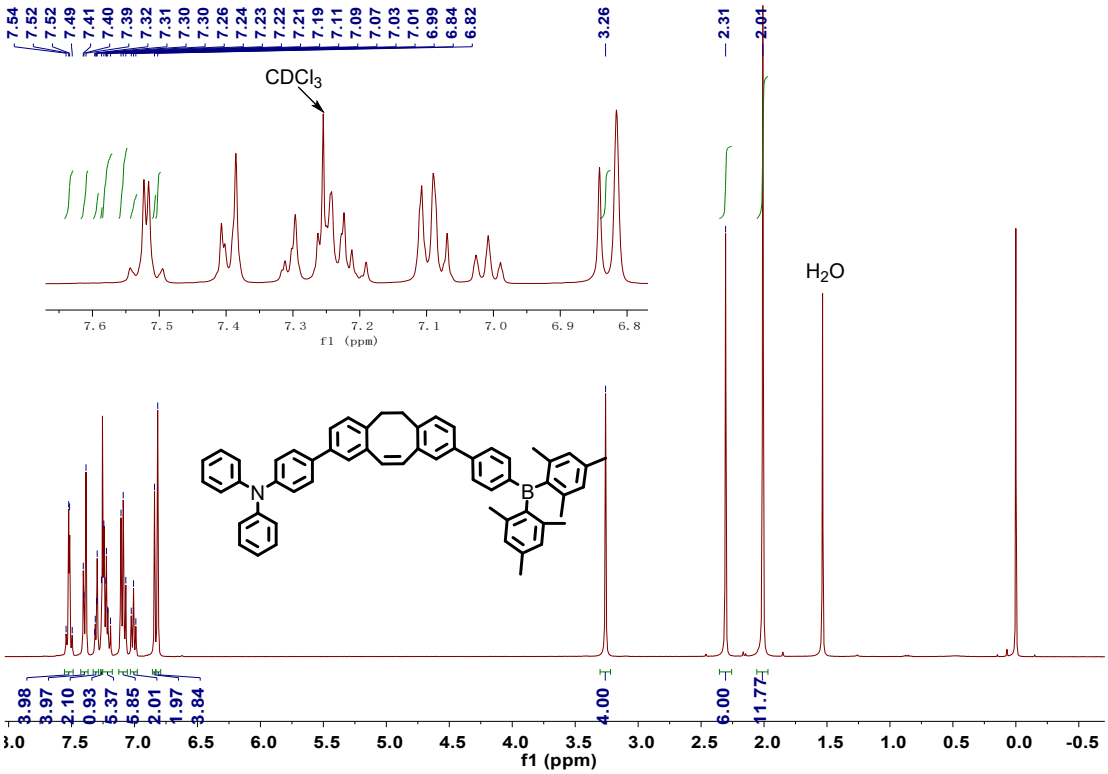

Figure S25. ^{1}H NMR (400 MHz, $CDCl_3$) spectrum of **M2**.

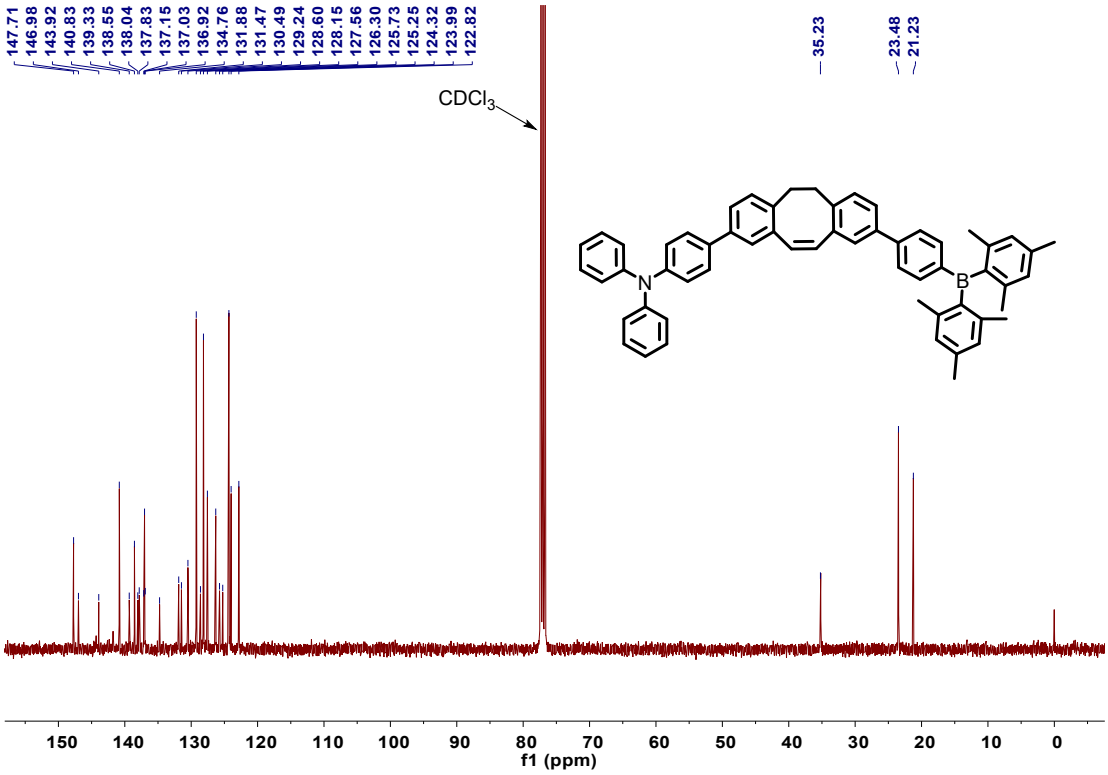

Figure S26. ^{13}C NMR (101 MHz, $CDCl_3$) spectrum of **M2**.

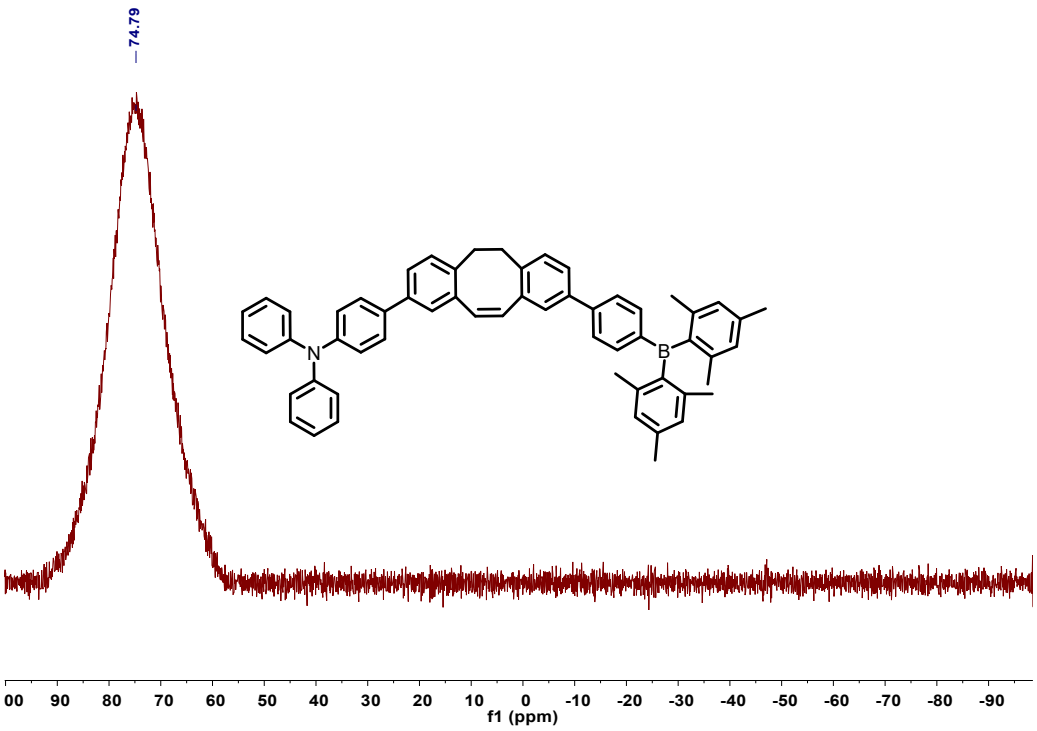

Figure S27.[11]B NMR (225 MHz, C_6D_6) spectrum of **M2**.

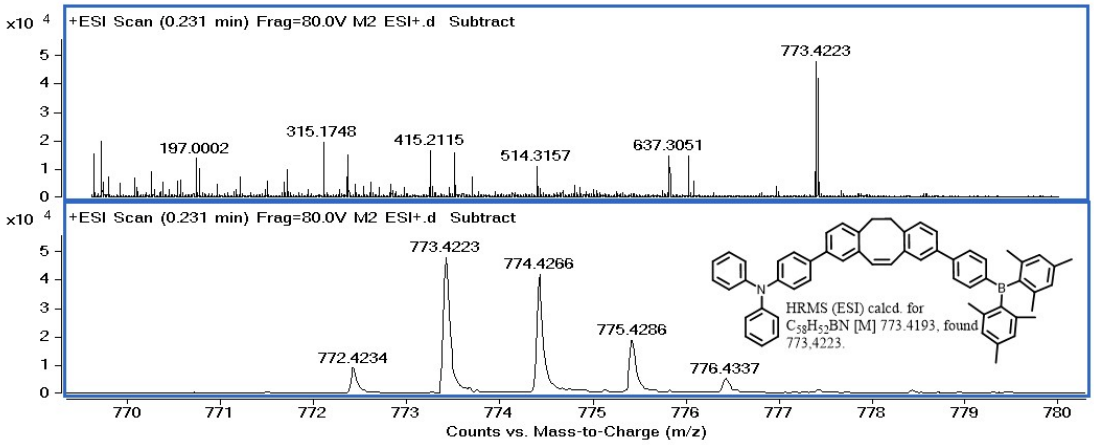

Figure S28. HRMS spectrum for **M2**.

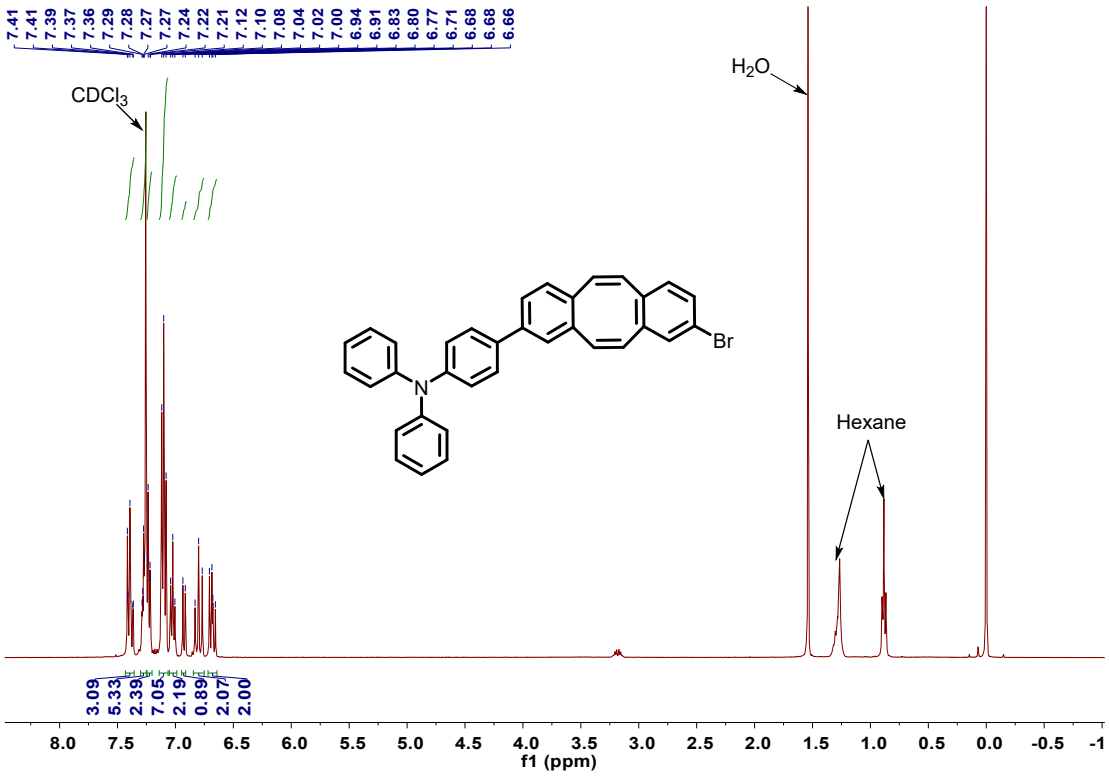

Figure S29. ^{1}H NMR (400 MHz, $CDCl_3$) spectrum of **14**.

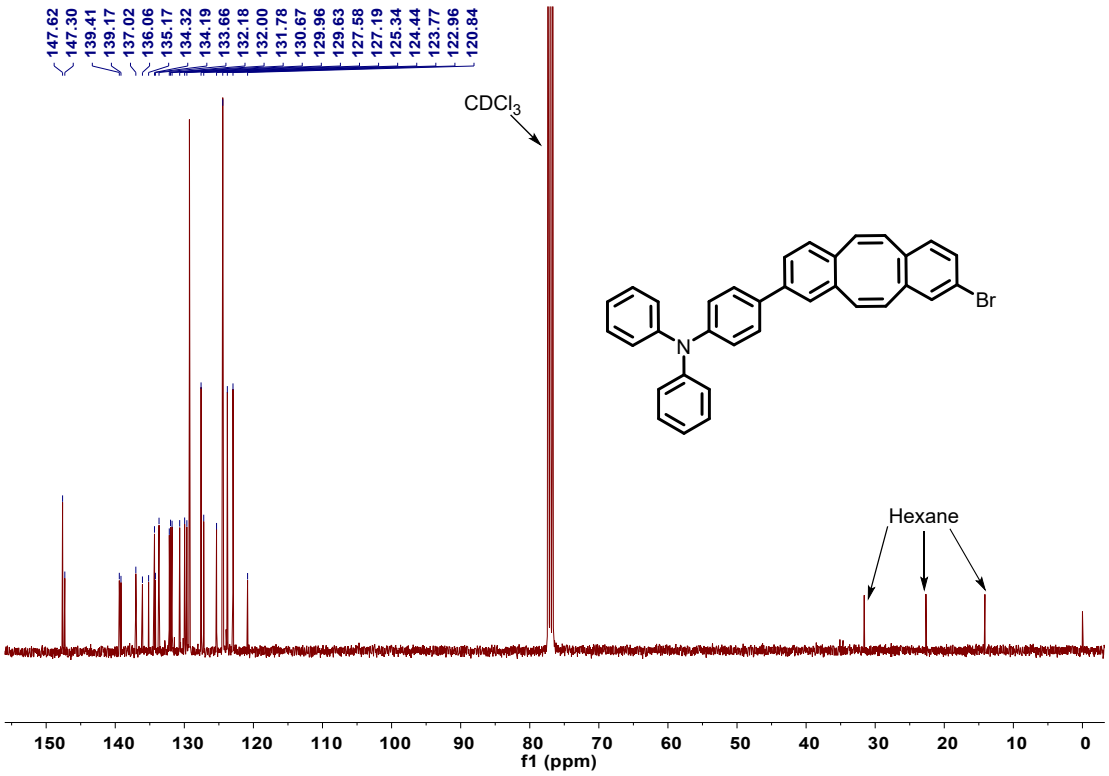

Figure S30. ^{13}C NMR (101 MHz, $CDCl_3$) spectrum of **14**.

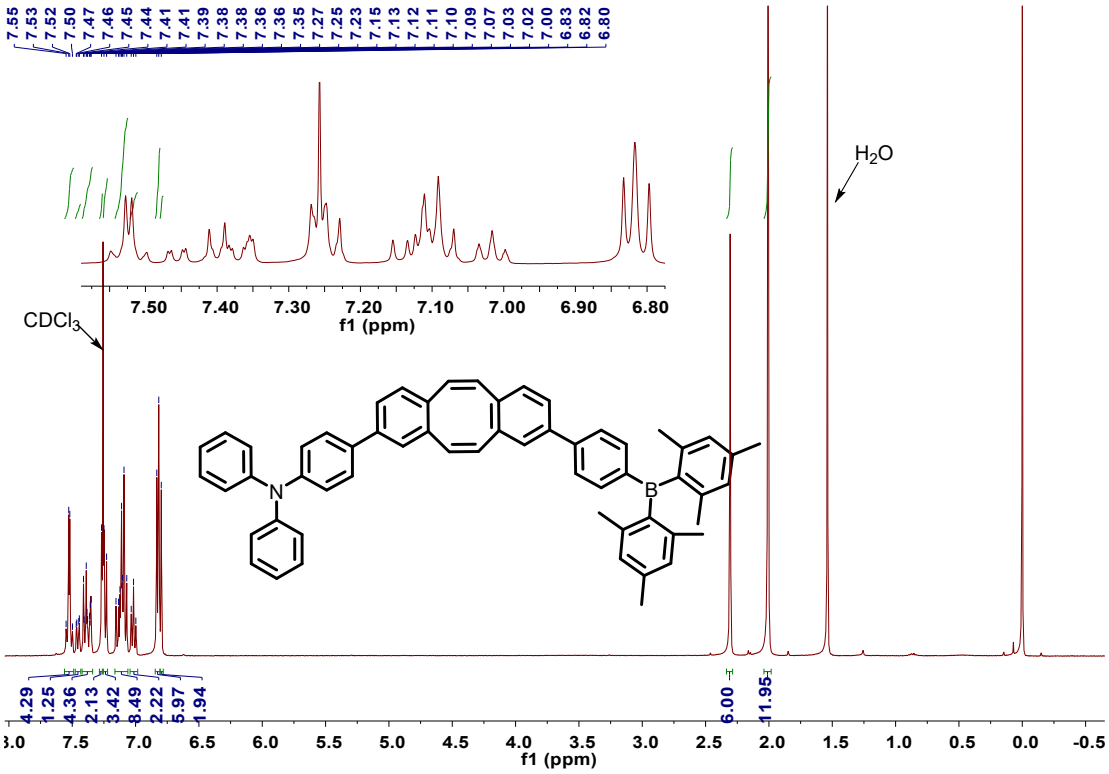

Figure S31. ^{1}H NMR (400 MHz, $CDCl_3$) spectrum of **M3**.

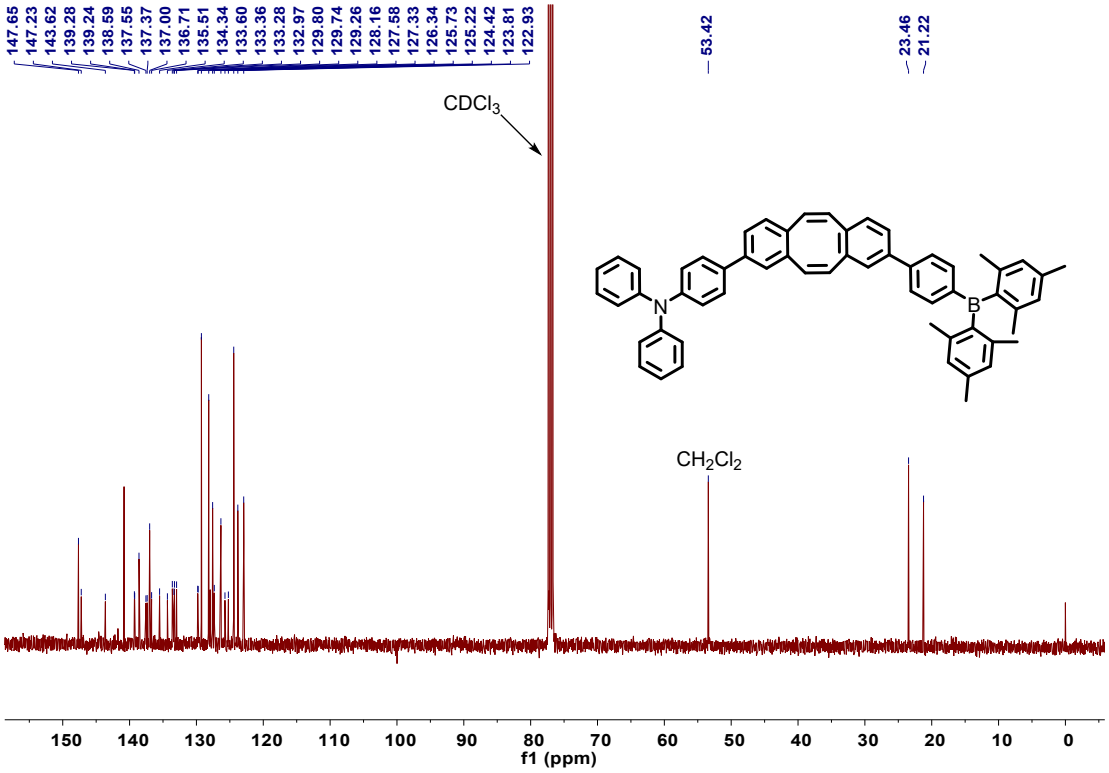

Figure S32. ^{13}C NMR (101 MHz, $CDCl_3$) spectrum of **M3**.

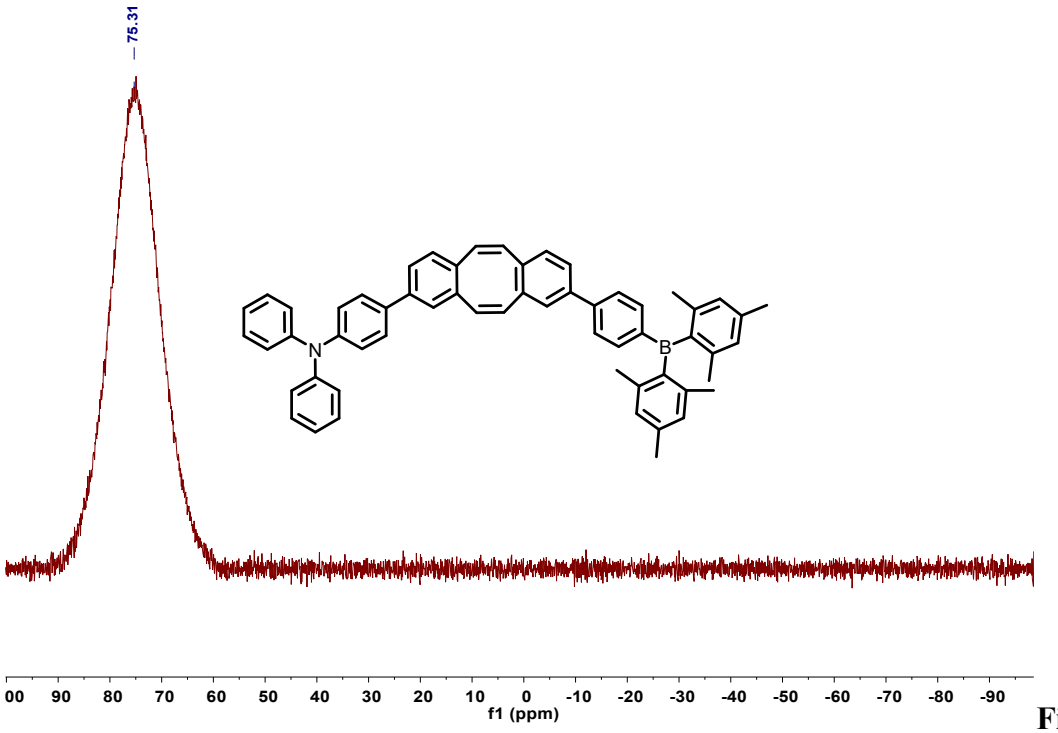

Figure S33.^{11}B NMR (225 MHz, C_6D_6) spectrum of **M3**.

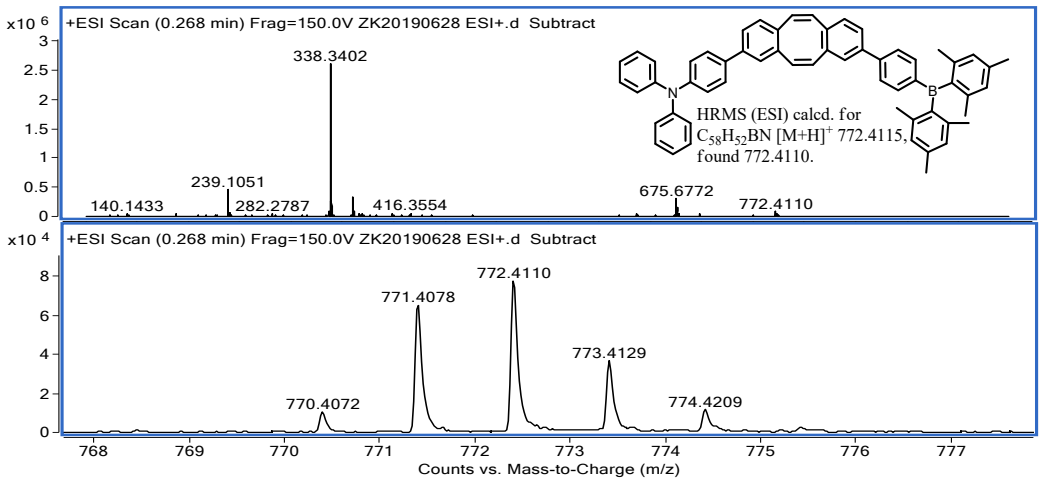

Figure S34. HRMS spectrum for **M3**.

4. XRD Measurements

Table S1. Crystallographic data and structure refinement for **M2**.

Compound	M2
Empirical formula	$C_{58}H_{52}BN$
Formula weight	773.81
Temperature/K	180.0
Crystal system	triclinic
Space group	P-1
Unit cell	a = 11.6873(6) Å; b = 13.6233(7) Å; c = 17.5745(10) Å. α = 74.330(2)°; β= 74.445(2)°; γ= 67.948(2)°.
Volume/Å^3	2453.1(2)
Z	2
ρ_{calc}g/cm^3	1.048
μ/mm^{-1}	0.059
F (000)	824.0
Crystal size/mm^3	0.41 × 0.26 × 0.22
Radiation	MoKα (λ = 0.71073)
2θ range for data collection/°	4.9 to 50
Index ranges	-13 ≤ h ≤ 13, -16 ≤ k ≤ 16, -20 ≤ l ≤ 20
Reflections collected	27498
Independent reflections	8569 [R_{int} = 0.0456, R_{sigma} = 0.0537]
Data/restraints/parameters	8569/0/547
Goodness-of-fit on F^2	1.031
Final R indexes [I>=2σ (I)]	R_1 = 0.0515, wR_2 = 0.1251
Final R indexes [all data]	R_1 = 0.0857, wR_2 = 0.1441
Largest diff. peak/hole (e. Å^{-3})	0.22/-0.26

Table S2. Selected bond distances (Å) from X-ray data for **M2.**

Bond	Bond Length/Å	Bond	Length/Å
N(1)-C(4)	1.421(3)	B(1)- C(20)	1.561(3)
N(1)-C(5)	1.418(2)	B(1)- C(22)	1.581(3)
N(1)-C(30)	1.416(3)	B(1)- C(37)	1.578(3)

Table S3. Selected bond angles (°) from X-ray data for **M2.**

	Bond Angle		Bond Angle
C(5)-N(1)-C(4)	119.23(16)	C(20)-B(1)-C(22)	118.96(17)
C(30)-N(1)-C(4)	119.00(16)	C(20)-B(1)-C(37)	117.65(17)
C(30)-N(1)-C(5)	120.04(17)	C(37)-B(1)-C(22)	123.37(17)

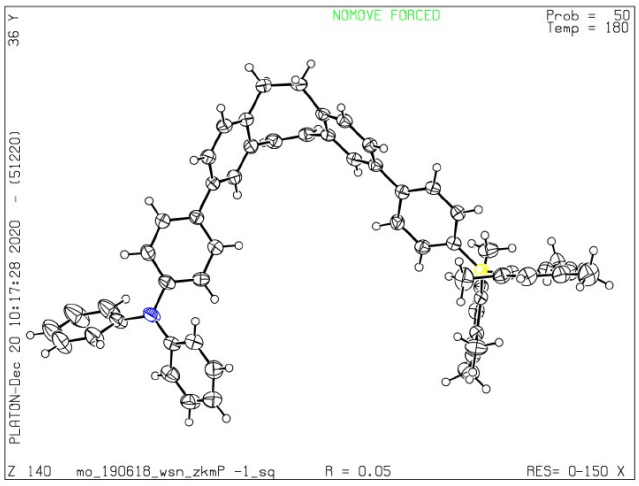

Figure S35. X-ray crystal structure of **M2** (50% thermal ellipsoids). Color code: N (Blue) and B (yellow).

5. Spectral characterization

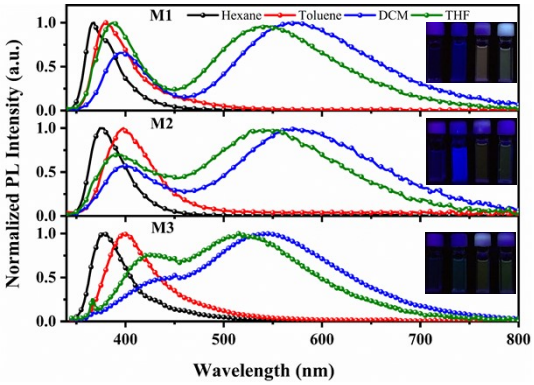

Figure S36. Emission spectra of **M1, M2** and **M3** in solvents (1.0×10^{-5} M) of different polarity in air at 298 K.

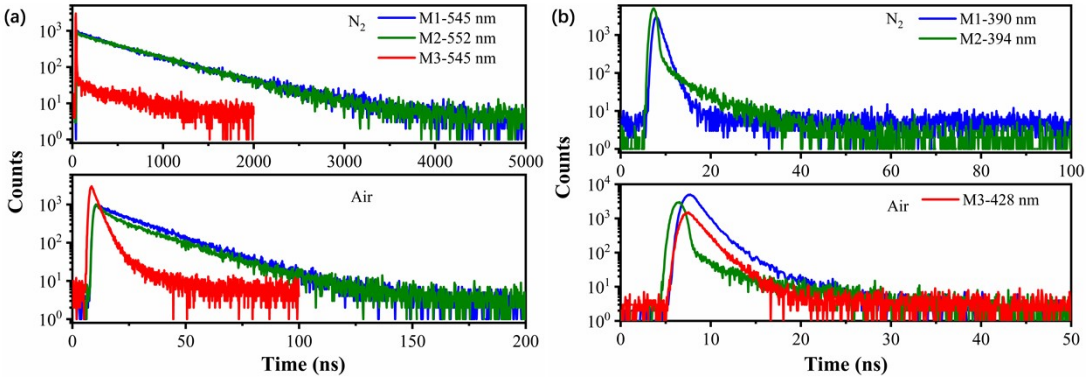

Figure S37. PL decay curves of **M1, M2** and **M3** in THF (1.0×10^{-5} M) under N_2 and air atmosphere at 298 K.

Table S4. Summary of absorption and emission properties of **M1**, **M2** and **M3** in THF (1.0×10^{-5} M) under N_2 at 298 K.

	λ_{abs} [nm]	λ_{em} [nm]	φ_{PL} (%)	τ[ns]			Rel %	χ^2
				τ_1	τ_2	$\tau_{ave.}$		
M1	329	390	15	1.34		1.34	100	1.297
		545		254.70	727.80	640.47	18.46/81.54	1.029
M2	331	394	10	0.30	3.88	2.04	51.52/48.48	1.15
		552		319.60	549.80	527.81	9.55/90.45	1.083
M3	331	545	3	4.00	555.80	349.81	37.33/62.67	1.214

Table S5. Summary of emission photophysical propertie of **M1**, **M2** and **M3** in THF (1.0×10^{-5} M) under air at 298 K.

	λ_{em} [nm]	φ_{PL} (%)	τ[ns]			Rel %	χ^2
			τ_1	τ_2	$\tau_{ave.}$		
M1	390	3	1.14	3.33	1.63	77.98/22.02	1.09
	545		20.52		20.52	100	1.294
M2	394	1	0.36	6.18	2.86	57.08/42.92	1.248
	552		4.18	22.32	20.01	12.74/82.26	1.116
M3	428	1	1.40	2.95	1.53	87.77/12.23	1.255
	545		2.79	11.48	3.83	89.23/10.77	1.197

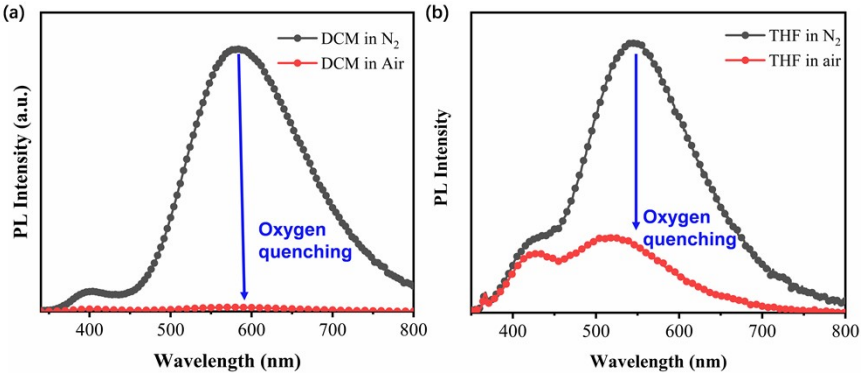

Figure S38. PL spectra of (a) **M2** (in DCM, 1.0×10^{-5} M), and (b) **M3** (in THF, 1.0×10^{-5} M) under N_2 and air atmosphere at 298 K.

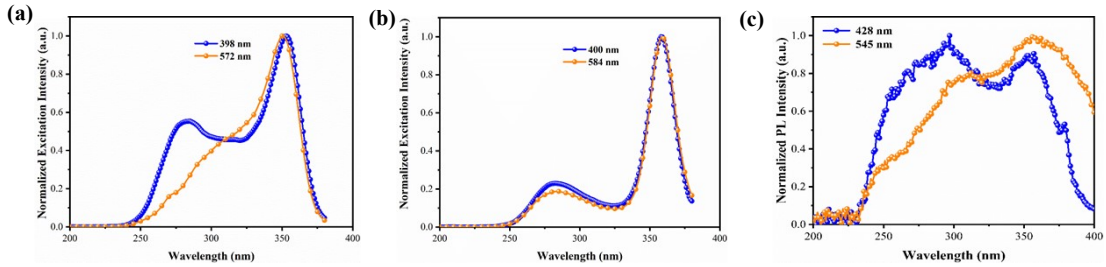

Figure S39. Excitation spectra of (a) **M1** (in DCM, 1.0×10^{-5} M) and (b) **M2** (in DCM, 1.0×10^{-5} M), and (c) **M3** (in THF, 1.0×10^{-5} M) under N_2 at 298 K.

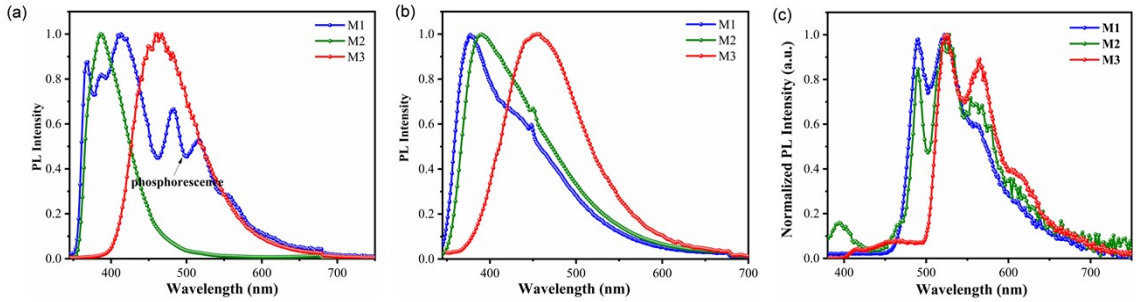

Figure S40. PL spectra of **M1**, **M2** and **M3** (a) in MTHF at 77 K and (b) 5% PMMA doped films, (c) phosphorescence spectra (77 K) in MTHF.

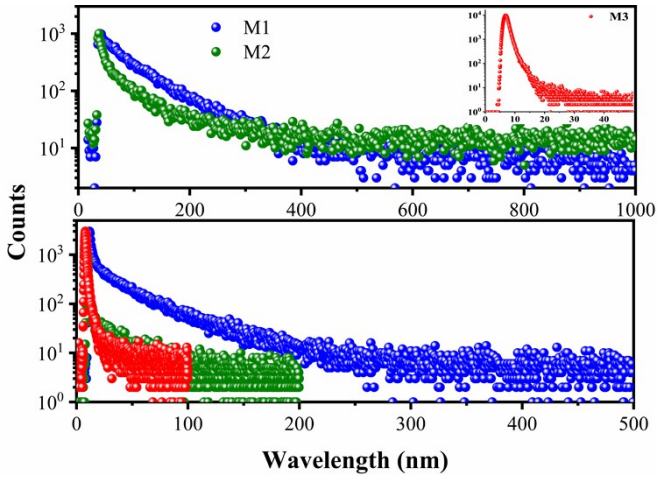

Figure S41. Transient PL decays of **M1**, **M2** and **M3** solid powder (top) and crystalline sample (bottom) in air at 298 K.

Table S6. PL decay curves of **M1**, **M2** and **M3** of solid powder (top) and crystalline sample (bottom) in air.

		λ_{max} [nm]	Φ_{PL} (%)	τ [ns]				Rel %	χ^2
				τ_1	τ_2	τ_3	$\tau_{ave.}$		
solid powder	**M1**	445	20	27.25	79.90		68.40	21.84/78.16	1.132
	M2	432	18	8.52	66.06		51.03	26.12/73.88	1.151
	M3	448	5	0.74	2.06	16.85	1.45	70.31/27.51/2.18	1.168
Crystalline sample	**M1**	430	22	1.51	15.74	51.50	34.08	14.71/28.15/57.14	1.112
	M2	425	20	1.06	27.14		15.67	43.99/56.01	1.225
	M3	460	6	0.79	3.02	24.46	3.95	61.09/28.24/10.67	1.275

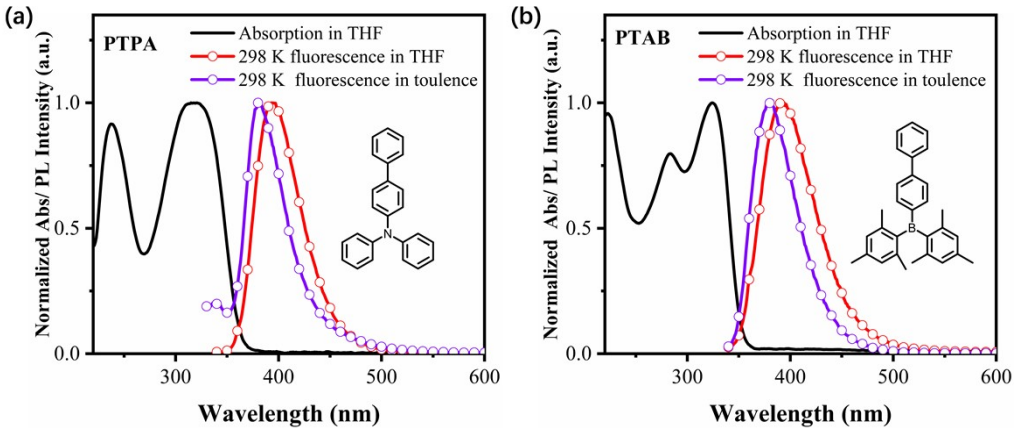

Figure S42. Absorption and emission spectra of **PTPA** and **PTAB** in THF and toluene (1×10^{-5} M) under N_2 at 298 K.

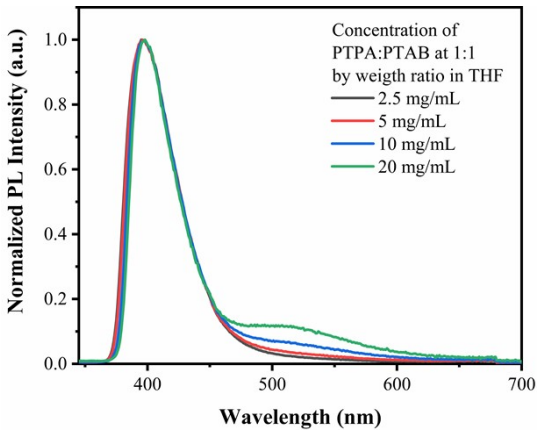

Figure S43. PL spectra of **PTPA/PTAB** mixture in THF with different concentrations under N_2 at 298 K.

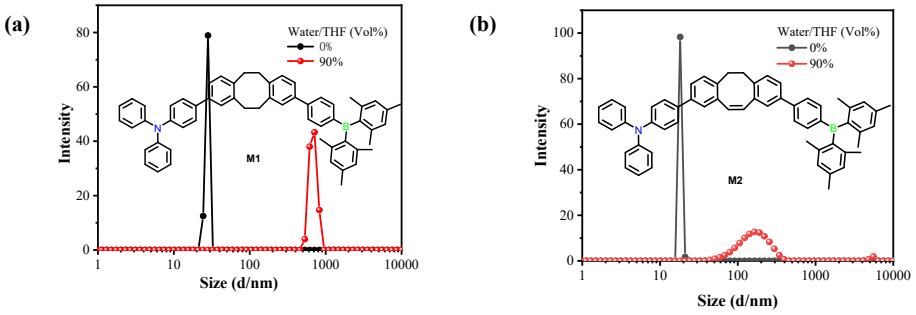

Z-Average Size (d/nm)	
0%	27.69
90%	684.70

Z-Average Size (d/nm)	
0%	18.22
90%	169.80

Figure S44. Dynamic Light Scattering (DLS) spectra of (a) **M1** and (b) **M2.**

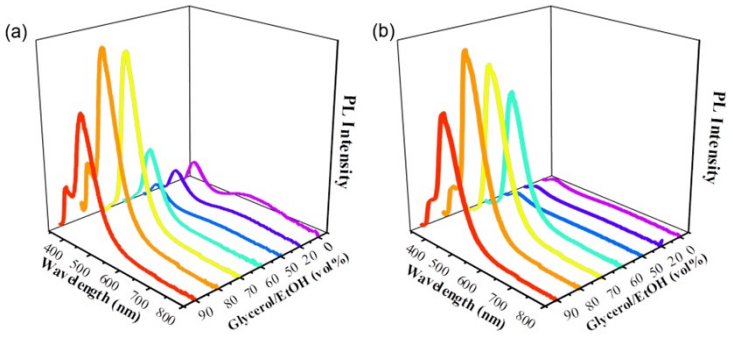

	0%	20%	50%	60%	70%	80%	90%
M1	391/605	391/625	394/624	446	445	372/445	372/445
M2	390/624	390/635	392/670	445	449	383/449	383/445

Figure S45. PL spectra of (a) **M1** and (b) **M2** in EtOH-glycerol mixtures (1.0×10^{-5} M) under N_2 at 298 K.

Table S7. Temperature-dependent photophysical properties and fitting results of temperature-dependent transient decay spectra of **M1** in MTHF (0.03 mM) under N_2.

T [K]	λ_{max} [nm]	τ [ns]			Rel %	χ^2	CIE [x,y]
		τ_1	τ_2	$\tau_{ave.}$			
150	628	2.99	598.40	584.83	2.28/97.72	1.177	[0.53,0.39]
180	608	196.40	925.40	786.37	19.07/80.93	1.225	[0.52,0.44]
210	575	20.00	775.30	767.24	1.07/98.93	1.240	[0.45,0.50]
270	538	13.41	658.00	653.65	0.67/99.33	1.102	[0.30,0.50]

300	518	3.90	503.10	499.97	0.63/99.37	0.906	[0.28,0.44]
330	497	10.00	365.9	364.06	0.52/99.48	1.132	[0.23,0.36]
345	491	10.00	307.9	304.94	0.99/99.01	1.175	[0.21,0.32]

Table S8. Temperature-dependent photophysical properties and fitting results of temperature-dependent transient decay spectra of **M2** in MTHF (0.03 mM) under N_2.

T [K]	λ_{max} [nm]	τ [ns]			Rel %	χ^2	CIE [x,y]
		τ_1	τ_2	$\tau_{ave.}$			
150	650	20	456.1	451.75	1/99	1.116	[0.52,0.34]
180	620	20	724.8	719.97	0.68/99.32	1.113	[0.52,0.43]
210	590	10.46	953.1	948.57	0.48/99.52	1.180	[0.48,0.48]
240	560	24.06	874.7	869.72	0.58/99.42	1.136	[0.42,0.51]
270	545	5.34	622.0	618.48	0.57/99.43	1.011	[0.35,0.49]
300	521	2.37	431.0	428.25	0.64/99.36	1.091	[0.28,0.43]
330	502	2.39	276.8	267.55	3.37/96.63	0.927	[0.22,0.31]
345	474	2.98	196.2	190.24	3.08/96.92	1.079	[0.20,0.24]

Table S9. Temperature-dependent photophysical properties and fitting results of temperature-dependent transient decay spectra of **M3** in MTHF (0.03 mM) under N_2.

T [K]	λ_{max} [nm]	τ [ns]			Rel %	χ^2	CIE [x,y]
		τ_1	τ_2	$\tau_{ave.}$			
150	630	6.66	337.1	182.62	46.75/53.25	1.372	[0.46,0.38]
180	615	5.97	570.30	314.51	45.33/54.67	1.191	[0.46,0.40]
210	582	4.44	700.60	407.34	42.13/57.87	1.229	[0.44,0.45]
240	560	3.90	707.60	444.76	37.35/62.65	1.151	[0.39,0.48]
270	535	3.57	546.10	332.85	39.31/60.69	1.029	[0.33,0.46]
300	518	3.07	360.40	201.75	44.40/55.60	1.023	[0.27,0.41]
330	495	2.63	222.20	110.09	51.05/48.95	1.056	[0.22,0.31]
345	485	2.48	174.10	74.72	57.91/42.09	1.073	[0.20,0.25]

6. Spectroscopic Tracking by ^{1}H NMR Measurements

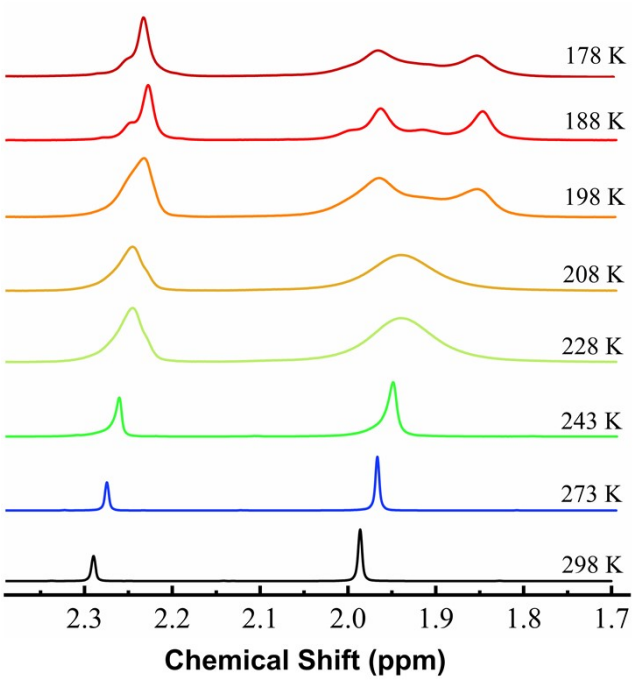

Figure S46. Variable-temperature ^{1}H NMR spectra of the methyl protons on Ar_3B of **M1** in CD_2Cl_2–CS_2 (4:1) at various temperatures

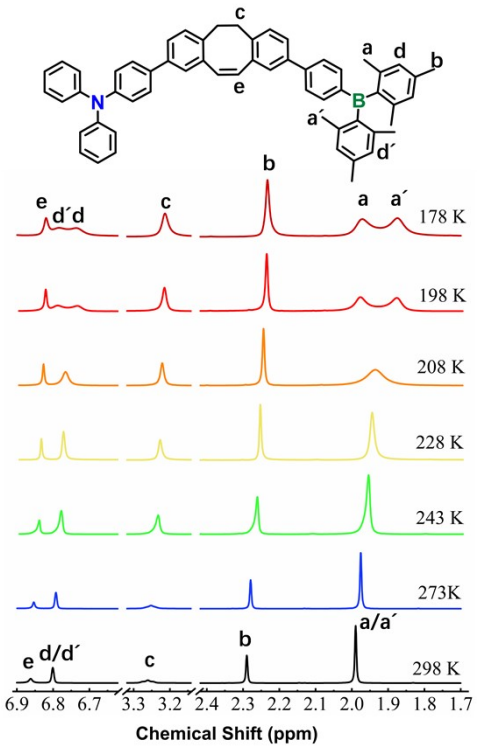

Figure S47. Variable-temperature ^{1}H NMR spectra of **M2** in CD_2Cl_2–CS2 (4:1) at various temperatures.

7. Transient absorption spectroscopy

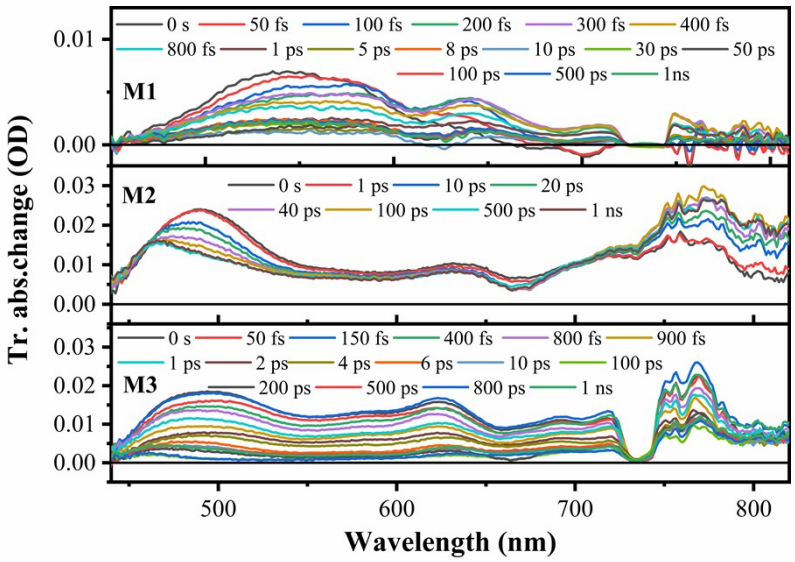

Figure S48. Femtosecond time-resolved absorption spectra of **M1**, **M2** and **M3** in MTHF at selected delay times, obtained upon 330 nm photoexcitation.

8. DFT and TD-DFT Computations

DFT and TD-DFT calculations were performed using the Gaussian 09 suite of programs.[3] Geometry optimizations and vertical excitations of all compounds were obtained at the B3LYP/6-31G*, CAM-B3LYP/6-31G* and B3LYP/6-311G** level of theory,[4,5] and the resulting structures were confirmed to be stationary points through vibrational frequency analysis.

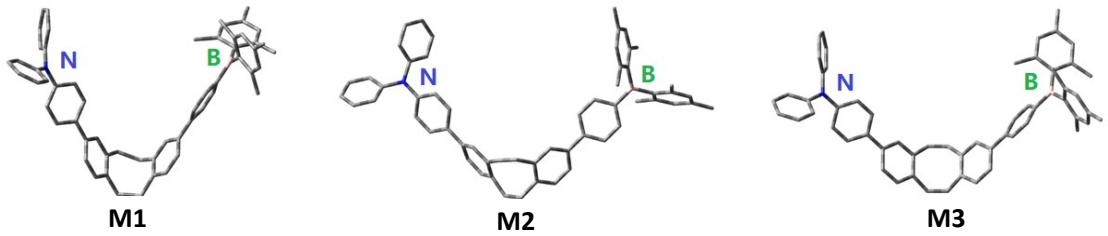

Figure S49. DFT optimized structures of **M1-M3** (B3LYP/6-31G*).

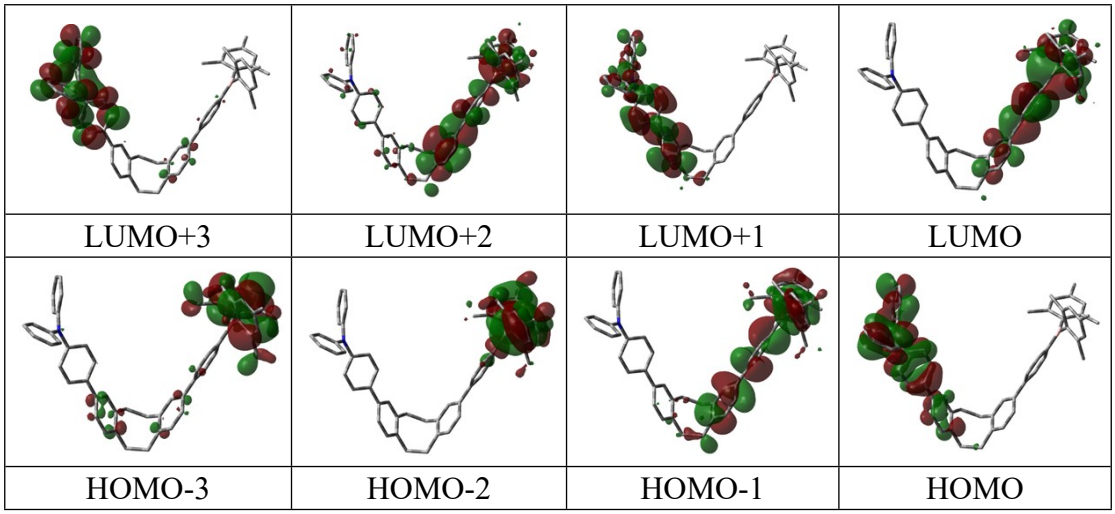

Figure S50. Molecular orbitals contributing to the DFT calculated transitions of **M1** (iso = 0.02, B3LYP/6-31G*).

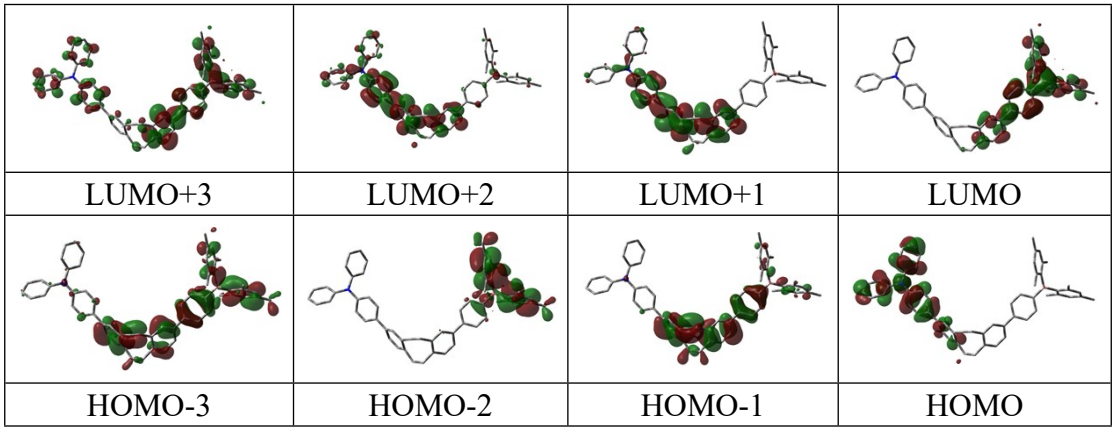

Figure S51. Molecular orbitals contributing to the DFT calculated transitions of **M2** (iso = 0.02, B3LYP/6-31G*).

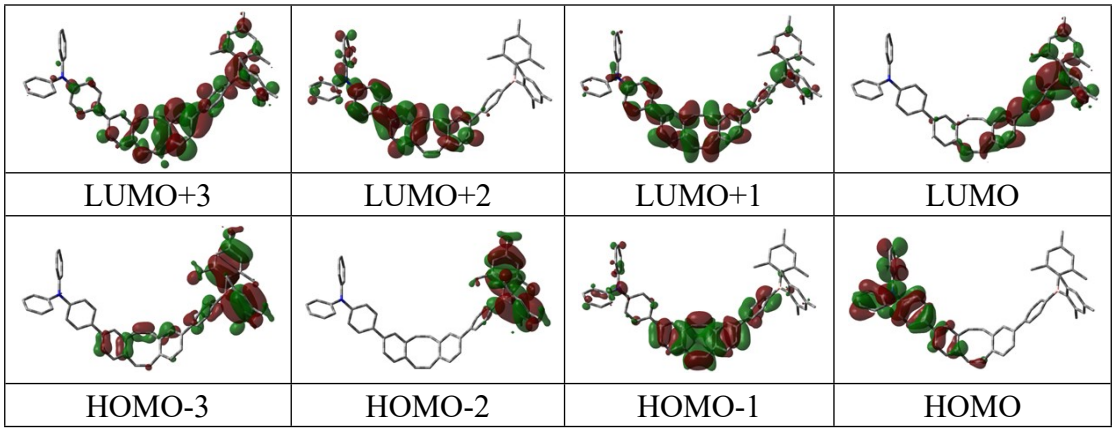

Figure S52. Molecular orbitals contributing to the DFT calculated transitions of **M3** (iso = 0.02, B3LYP/6-31G*).

Table S10. Comparison of the TD-DFT calculations (B3LYP, 6-311G**) for **M1–M3.**

Compound	Transition	λ, nm (eV)	Oscillator Strength, *f*	Orbital Contributions
M1	$S_0 \rightarrow S_1$	421 (2.95)	0.0007	HOMO→LUMO (100%)
	$S_0 \rightarrow S_2$	352 (3.52)	0.0733	HOMO-2→LUMO (96%)
	$S_0 \rightarrow S_3$	349 (3.55)	0.3948	HOMO-1→LUMO (46%) HOMO→LUMO+1 (42%)
	$S_0 \rightarrow S_4$	343 (3.62)	0.5457	HOMO-3→LUMO (12%) HOMO-1→LUMO (27%) HOMO→LUMO+1 (53%)
	$S_0 \rightarrow S_5$	334 (3.71)	0.0793	HOMO-3→LUMO (76%)
M2	$S_0 \rightarrow S_1$	415 (2.99)	0.0000	HOMO→LUMO (100%)
	$S_0 \rightarrow S_2$	357 (3.47)	0.2313	HOMO-2→LUMO (35%) HOMO→LUMO+1 (56%)
	$S_0 \rightarrow S_3$	357 (3.47)	0.3627	HOMO-2→LUMO (61%) HOMO→LUMO+1 (29%)
	$S_0 \rightarrow S_4$	348 (3.56)	0.3025	HOMO-3→LUMO (41%) HOMO-1→LUMO (36%)
	$S_0 \rightarrow S_5$	336 (3.69)	0.1237	HOMO-4→LUMO (69%)
M3	$S_0 \rightarrow S_1$	426 (2.91)	0.0782	HOMO→LUMO (97%)
	$S_0 \rightarrow S_2$	375 (3.30)	0.5062	HOMO-1→LUMO (12%) HOMO→LUMO+1 (80%)
	$S_0 \rightarrow S_3$	360 (3.44)	0.0934	HOMO-2→LUMO (86%)
	$S_0 \rightarrow S_4$	359 (3.45)	0.3557	HOMO-1→LUMO (62%) HOMO→LUMO+1 (14%)
	$S_0 \rightarrow S_5$	343 (3.61)	0.0039	HOMO-3→LUMO (75%)

Table S11. Coordinates (Å) for the optimized structure (B3LYP, 6-31G*) of **M1**.

atom	X	Y	Z	atom	X	Y	Z
C	0.307328	5.174501	-1.81485	H	3.498877	3.164358	1.380381
C	1.219795	4.125619	-1.75190	H	5.070789	1.282140	1.554201
C	1.581241	3.571381	-0.51550	H	3.491482	-0.37439	-2.08245
C	0.985171	4.110087	0.635024	H	1.854959	1.455627	-2.20629
C	0.060898	5.15694	0.582898	H	5.72380	-4.87294	-2.75821
C	-0.28599	5.71393	-0.666140	H	7.035205	-1.25834	-4.63821
C	-2.84748	4.55340	1.040113	H	9.135822	-1.37186	2.812425
C	-3.39331	3.26561	1.038783	H	5.251489	-2.08758	4.461043
C	-4.28016	2.814836	0.047972	H	-6.77823	1.981196	-0.6752
C	-4.62267	3.713933	-0.97281	H	-7.68731	-0.30171	-0.63188

C	-4.08832	4.998607	-0.98630	H	-3.94745	-1.76245	0.898692
C	-3.19979	5.43965	0.000897	H	-3.03329	0.517706	0.842606
C	-1.23558	6.892304	-0.82223	H	-5.7773	-5.11576	0.066859
C	-2.61000	6.828227	-0.08548	H	-5.32367	-6.59496	1.995631
C	2.553299	2.455056	-0.42543	H	-5.40166	-5.69277	4.316543
C	-4.83078	1.438645	0.081172	H	-5.95582	-3.29036	4.675298
C	3.476811	2.376001	0.632771	H	-6.43918	-1.82101	2.746265
C	4.375377	1.318243	0.719864	H	-8.64519	-3.97668	0.354974
C	4.422265	0.296207	-0.25315	H	-10.024	-4.80746	-1.52163
C	3.497175	0.395823	-1.31537	H	-9.39462	-4.27923	-3.87344
C	2.579119	1.437113	-1.39633	H	-7.35334	-2.92084	-4.316
C	5.805999	-1.69961	-1.47307	H	-5.95874	-2.11845	-2.43841
C	6.089062	-1.23452	1.2515	B	5.443346	-0.89161	-0.157
C	5.608626	-3.10645	-1.54553	C	8.447344	-0.82342	0.309837
C	5.900964	-3.79922	-2.72276	H	8.325895	-1.48594	-0.55231
C	6.42017	-3.15853	-3.85144	H	8.285797	0.201363	-0.04789
C	6.624923	-1.78148	-3.77556	H	9.488171	-0.88811	0.642882
C	6.316868	-1.04558	-2.62444	C	3.787044	-1.75127	2.29865
C	7.501299	-1.1831	1.437866	H	3.289092	-1.2695	3.148466
C	8.054947	-1.43168	2.694243	H	3.35135	-1.34382	1.385385
C	7.266789	-1.75501	3.804712	H	3.528053	-2.81784	2.341588
C	5.889074	-1.82332	3.618329	C	7.89572	-2.00893	5.154345
C	5.291293	-1.56709	2.375803	H	8.727714	-2.71974	5.081563
C	-6.14122	1.16427	-0.34749	H	8.301984	-1.0846	5.585901
C	-6.66445	-0.12377	-0.315300	H	7.168258	-2.41337	5.865516
C	-5.88478	-1.20029	0.137666	C	5.045458	-3.89764	-0.38151
C	-4.57161	-0.94086	0.56191	H	5.685522	-3.82955	0.50395
C	-4.06325	0.353193	0.538623	H	4.051136	-3.54111	-0.08628
N	-6.41066	-2.51875	0.165793	H	4.946307	-4.95557	-0.64511
C	-6.14057	-3.36731	1.274389	C	6.772878	-3.93847	-5.09603
C	-7.20747	-2.99028	-0.91302	H	6.03565	-4.72334	-5.29977
C	-5.82268	-4.72095	1.076872	H	6.827218	-3.28775	-5.9751
C	-5.56839	-5.54998	2.167783	H	7.748644	-4.43247	-4.99382
C	-5.60754	-5.04497	3.469213	C	6.572274	0.450629	-2.679
C	-5.91416	-3.69715	3.668164	H	5.708294	0.988414	-3.0887
C	-6.18776	-2.86443	2.584881	H	6.775153	0.886864	-1.69844
C	-8.3611	-3.75314	-0.66841	H	7.428777	0.669475	-3.32644
C	-9.13431	-4.21881	-1.7301	C	-0.58273	5.641262	1.862982
C	-8.78532	-3.92017	-3.04892	C	-1.94048	4.948648	2.197824
C	-7.64325	-3.15506	-3.29492	H	-1.72263	4.036984	2.765001

C	-6.85342	-2.7002	-2.24085	H	0.095833	5.455882	2.703951
H	0.053126	5.5945	-2.78557	H	-3.30206	7.484763	-0.62612
H	1.674904	3.753756	-2.6655	H	-2.51946	7.256624	0.917259
H	1.228356	3.680972	1.604455	H	-0.72868	7.818131	-0.51123
H	-3.13943	2.594303	1.855419	H	-1.43257	7.008854	-1.8938
H	-5.2856	3.398031	-1.77334	H	-0.71343	6.726828	1.8232
H	-4.35961	5.679377	-1.7909	H	-2.49043	5.60403	2.889568

Table S12. Coordinates (Å) for the optimized structure (B3LYP, 6-31G*) of **M2**.

atom	X	Y	Z	atom	X	Y	Z
C	-3.5721	4.419388	1.166373	H	-7.14667	2.537407	1.307659
C	-4.50074	3.39336	1.25417	H	-8.79461	0.719905	1.419605
C	-4.65838	2.491011	0.189655	H	-6.11637	-1.84214	-0.75619
C	-3.83107	2.67266	-0.92133	H	-4.44139	-0.04585	-0.80929
C	-2.85291	3.685181	-1.01347	H	-8.73439	-6.25418	-0.46463
C	-2.73969	4.611285	0.048814	H	-5.97389	-4.89137	2.539274
C	0.339706	3.821368	-1.46106	H	-12.9752	-2.26935	1.473536
C	1.383043	2.891286	-1.34517	H	-11.9965	0.444439	-1.71679
C	2.431959	3.058118	-0.43162	H	5.082192	3.496919	0.02925
C	2.426708	4.216859	0.364513	H	6.870268	1.827561	0.259468
C	1.416137	5.162784	0.231717	H	4.040638	-1.31282	-0.51055
C	0.363223	4.99048	-0.67573	H	2.23126	0.345614	-0.63268
C	-1.90775	5.888395	0.090176	H	6.530303	-5.70973	-0.13414
C	-0.69417	6.055556	-0.8371	H	6.000612	-3.6545	-3.85037
C	-5.65749	1.396391	0.23971	H	11.45699	-0.33127	0.549384
C	3.51602	2.051804	-0.31839	H	9.004592	0.368221	3.986456
C	-6.90301	1.575081	0.866071	C	-2.05675	3.608224	-2.26691
C	-7.8435	0.552509	0.924449	C	-0.72488	3.583565	-2.45546
C	-7.57985	-0.69559	0.336609	H	-0.37941	3.322483	-3.45628
C	-6.34181	-0.88393	-0.29922	H	-2.66029	3.362882	-3.14111
C	-5.40092	0.139653	-0.33475	H	-0.25282	7.035098	-0.61359
C	-8.12278	-3.08107	0.613314	H	-1.02827	6.091467	-1.8781
C	-9.92018	-1.44896	0.20919	H	-2.58836	6.732617	-0.10048
C	-8.6879	-4.13631	-0.12093	H	-1.56457	6.021221	1.124501
C	-8.2859	-5.44995	0.112903	B	6.759713	-0.94748	-0.00391
C	-7.30433	-5.7341	1.064703	N	-8.53932	-1.7401	0.386057
C	-6.73376	-4.68575	1.789777	H	-9.59709	-0.07124	-1.41711
C	-7.14262	-3.37069	1.576344	H	-10.5727	-2.75843	1.792415
C	-10.8878	-2.06341	1.020581	H	-13.7073	-0.65676	-0.27877
C	-12.2405	-1.78411	0.836164	H	-6.70642	-2.56116	2.152894

C	-12.6524	-0.87738	-0.14282	H	-9.44118	-3.91939	-0.87158
C	-11.6918	-0.25784	-0.94515	H	-6.98819	-6.75862	1.239087
C	-10.338	-0.54483	-0.78088	C	6.62784	-0.12547	2.938231
C	4.843373	2.440632	-0.06065	H	6.159893	0.859347	2.820461
C	5.856093	1.494128	0.05353	H	5.899884	-0.86083	2.58583
C	5.610481	0.114369	-0.11231	H	6.77572	-0.29153	4.010891
C	4.2765	-0.25937	-0.38163	C	9.573139	-1.02234	-1.1892
C	3.252502	0.677945	-0.46755	H	9.165604	-2.01211	-1.41549
C	6.585204	-2.34021	-0.74248	H	9.095119	-0.3138	-1.87735
C	8.054411	-0.58875	0.838783	H	10.6414	-1.03311	-1.42812
C	6.6675	-3.57004	-0.03332	C	11.6058	0.450504	3.158674
C	6.480801	-4.78274	-0.70309	H	12.4685	-0.165	2.879866
C	6.242282	-4.84214	-2.07833	H	11.88827	1.497901	2.985665
C	6.176759	-3.63579	-2.7759	H	11.43779	0.332332	4.234339
C	6.327508	-2.39899	-2.13833	C	6.91708	-3.62242	1.460917
C	9.352675	-0.63693	0.260012	H	7.850835	-3.12315	1.736378
C	10.47533	-0.29557	1.019152	H	6.113839	-3.13538	2.027966
C	10.37802	0.076185	2.362527	H	6.973167	-4.65943	1.807106
C	9.106461	0.102622	2.935239	C	6.22257	-1.15711	-3.00637
C	7.953814	-0.20282	2.201931	H	5.210028	-0.7369	-2.98763
H	-3.483	5.114883	1.998514	H	6.898189	-0.35809	-2.6888
H	-5.09439	3.280114	2.156892	H	6.459695	-1.39789	-4.04827
H	-3.94164	1.999869	-1.76798	C	6.092439	-6.16736	-2.78751
H	1.377772	2.020785	-1.9962	H	7.071471	-6.60645	-3.02292
H	3.213804	4.370636	1.097157	H	5.554386	-6.89478	-2.16934
H	1.445288	6.062601	0.842991	H	5.549485	-6.0572	-3.73218

Table S13. Coordinates (Å) for the optimized structure (B3LYP, 6-31G*) of **3**.

atom	X	Y	Z	atom	X	Y	Z
C	-1.28806	5.133949	0.138039	H	5.568833	3.851663	1.213552
C	-2.30964	4.211864	0.320222	H	4.014553	5.713434	0.816226
C	-2.38578	3.065098	-0.48895	H	-3.68558	1.653978	-2.42972
C	-1.39976	2.898344	-1.46913	H	-5.45147	-0.02868	-2.14063
C	-0.34002	3.802066	-1.64256	H	-5.39618	0.637883	2.103884
C	-0.27715	4.947643	-0.82181	H	-3.55662	2.243475	1.828913
C	2.866161	3.593097	-1.5798	H	-8.72304	-2.60119	4.167008
C	3.795155	2.562154	-1.37129	H	-9.78204	1.387093	3.033853
C	4.773269	2.611499	-0.36939	H	-9.16664	-3.33367	-3.10773
C	4.83234	3.774023	0.418885	H	-5.12655	-4.55956	-2.40689
C	3.943673	4.818285	0.202667	H	7.414827	2.734743	0.316132

C	2.934008	4.74914	-0.77387	H	8.977648	0.872928	0.663732
C	0.731058	6.02091	-0.95993	H	5.844602	-1.92654	-0.24311
C	2.070705	5.937916	-0.9393	H	4.280172	-0.06387	-0.58593
C	-3.47831	2.076265	-0.32221	H	8.604325	-4.30138	1.186117
C	5.71812	1.489143	-0.16383	H	8.556386	-6.27684	-0.30094
C	-4.03717	1.413328	-1.4301	H	8.290332	-5.99023	-2.76129
C	-5.04793	0.472662	-1.26441	H	8.091465	-3.69536	-3.70992
C	-5.57845	0.162352	0.00588	H	8.172728	-1.72049	-2.22317
C	-5.02034	0.848167	1.105559	H	10.9989	-2.46867	0.316174
C	-3.98931	1.769334	0.952066	H	12.63983	-2.40231	2.165364
C	-7.66553	-0.79542	1.456426	H	11.9666	-1.56186	4.411848
C	-6.88561	-2.03069	-0.91112	H	9.622141	-0.80519	4.781391
C	-7.81548	-1.88338	2.358722	H	7.975726	-0.90195	2.938789
C	-8.63336	-1.75637	3.486179	B	-6.7224	-0.89658	0.185422
C	-9.34674	-0.58747	3.757903	C	-9.32146	-1.34334	-1.35665
C	-9.21789	0.472236	2.858505	H	-9.60103	-1.32347	-0.29944
C	-8.3874	0.397235	1.735322	H	-9.14112	-0.30425	-1.66113
C	-8.11053	-2.21981	-1.60723	H	-10.1836	-1.70077	-1.92877
C	-8.22009	-3.21531	-2.58285	C	-4.44959	-2.80027	-0.55055
C	-7.15894	-4.06791	-2.8954	H	-3.81453	-2.03655	-1.01439
C	-5.96282	-3.89419	-2.19789	H	-4.5256	-2.54188	0.50954
C	-5.80254	-2.89215	-1.23441	H	-3.91989	-3.75631	-0.62169
C	7.054127	1.715275	0.210482	C	-7.29807	-5.12851	-3.96168
C	7.945858	0.66554	0.398888	H	-8.31328	-5.53968	-3.98878
C	7.527828	-0.66599	0.236827	H	-7.08873	-4.71958	-4.95959
C	6.192841	-0.90496	-0.12978	H	-6.60023	-5.95653	-3.79757
C	5.31417	0.153251	-0.33247	C	-7.08396	-3.19708	2.167295
N	8.430433	-1.74061	0.438898	H	-7.27854	-3.6345	1.183929
C	8.391671	-2.87642	-0.41704	H	-5.99685	-3.07532	2.255404
C	9.375575	-1.68981	1.501078	H	-7.38859	-3.92341	2.927589
C	8.499287	-4.17192	0.113621	C	-10.214	-0.4681	4.988625
C	8.471848	-5.28142	-0.7292	H	-9.64585	-0.06483	5.838071
C	8.318664	-5.12272	-2.10815	H	-11.0617	0.204679	4.818773
C	8.202868	-3.83572	-2.63785	H	-10.6093	-1.44191	5.297307
C	8.248094	-2.71927	-1.80502	C	-8.32798	1.619957	0.836361
C	10.6993	-2.11118	1.296219	H	-7.44996	2.238834	1.054124
C	11.61949	-2.0720	2.342067	H	-8.27493	1.364082	-0.22583
C	11.24481	-1.59743	3.600842	H	-9.21578	2.244314	0.982653
C	9.931239	-1.169600	3.805117	C	0.601539	3.524069	-2.75155
C	8.999074	-1.22207	2.770534	C	1.939001	3.435253	-2.72426

H	-1.26492	6.031506	0.751565	H	2.612104	6.884653	-0.95159
H	-3.07743	4.400944	1.064806	H	0.309901	7.026574	-0.98745
H	-1.43316	2.019700	-2.10806	H	2.422773	3.120949	-3.64975
H	3.763108	1.701355	-2.03448	H	0.117816	3.273819	-3.69636

References:

[3] M. J. Frisch, G. W. Trucks, H. B. Schlegel, G. E. Scuseria, M. A. Robb, J. R. Cheeseman, G. Scalmani, V. Barone, B. Mennucci, G. A. H. Petersson, M. Nakatsuji, X. Caricato, H. P. F. Li, A. Hratchian, J. Izmaylov, G. Bloino, J. L. Zheng, M. Sonnenberg, M. Hada, K. Ehara, R. Toyota, J. Fukuda, M. Hasegawa, T. Ishida, Y. Nakajima, O. Honda, H. Kitao, T. Nakai, J. A. Vreven, J. E. Montgomery Jr., F. Peralta, M. Ogliaro, J. J. Bearpark, E. Heyd, K. N. Brothers, V. N. Kudin, T. Staroverov, R. Keith, J. Kobayashi, K. Normand, A. Raghavachari, J. C. Rendell, S. S. Burant, J. Iyengar, M. Tomasi, N. Cossi, J. M. Rega, M. Millam, J. E. Klene, J. B. Knox, V. Cross, C. Bakken, J. Adamo, R. Jaramillo, R. E. Gomperts, O. Stratmann, A. J. Yazyev, R. Austin, C. Cammi, J. W. Pomelli, R. L. Ochterski, K. Martin, V. G. Morokuma, G. A. Zakrzewski, P. Voth, J. J. Salvador, S. Dannenberg, A. D. Dapprich, O. Daniels, J. B. Farkas, J. V. Foresman, J. Ortiz, J. Cioslowski, D. J. Fox, Gaussian 09 Revision C.01, 2010.

[4] (a) C. Lee, W. Yang, R. G. Parr, *Phys. Rev. B,* **1988**, *37*, 785−789. (b) A. D. Becke, *J. Chem. Phys.* **1993**, *98*, 1372−1377. (c) A. D. Becke, *J. Chem. Phys.* **1993**, *98*, 5648−5652.

[5] (a) R. Ditchfield, W. J. Hehre, J. A. Pople, *J. Chem. Phys.* **1971**, *54*, 724–728. (b) A. D. McLean, G. S. Chandler, *J. Chem. Phys.* **1980**, *72*, 5639–5648.